Investors' Risk Attitudes and Option Prices

January 23, 2025

Abstract

This paper introduces a new economic theory of investment portfolios in incomplete markets to explore investors' risk attitudes and their influence option prices. The theory produces upper and lower bounds on prices, which vary with investors' higher-order risk attitudes and the distribution of the underlying asset return. We demonstrate that the range of admissible equilibrium option prices narrows as investors become averse to increasingly higher-order risks. Numerical analysis reveals that commonly observed implied volatility profiles, like smiles and smirks, emerge endogenously from the interplay between investors' aversion to downside risk, or prudence, and their beliefs about the concentration of tail risk in the underlying return distribution. However, we find that after accounting for prudence, higher-order attitudes like temperance have a negligible impact on option prices, irrespective of the balance between inside and outside risk.

Key words: Stochastic dominance, option pricing.

1 Introduction

It is well known that option prices in incomplete markets are governed by both investors' beliefs and their attitudes toward risk. A plot of implied volatilities across exercise prices (or IV profile) for a given tenor of options, for example, may be uniformly downward sloping or instead exhibit either a smile or a smirk, and whether or not these alternative patterns are evident depends on the interaction of these factors.[1] There is no doubt prices and IV profiles rise and fall together with the volatility of the underlying return. This relation follows from the convexity of options' payoffs. However there is little detailed or formal understanding of how investor beliefs regarding high-order moments of return, such as those represented by measures of skewness or kurtosis of a distribution, interact with risk attitudes to drive option prices. We introduce a theory of investment portfolios to study this issue.

The theory provides approximations of option prices and IV profiles without assuming a single agent pricing all assets. It produces upper and lower bounds, instead of identifying equilibrium values, where the bounds on option prices vary with the degree of high-order risk attitudes and with the moments of the underlying asset returns. The bounds represent moments of future option payoffs, using parametric stochastic discount factors. The environment allows multiple agents acting as marginal investors in options across exercise prices, with equilibrium values falling between the bounds. At the same time the range between the bounds can be sufficiently narrow to identify the global shape of the IV profile in equilibrium, suggesting how and why IV profiles vary with investor attitudes and beliefs.

Our bounds are stochastic dominance (SD) bounds that vary with investors' commonly-held risk attitudes, and our model is built on a collection of nested classes of investors $\mathbf{M}_n$, one class for each integer $n \geq 2$, with $\mathbf{M}_{n+1} \subset \mathbf{M}_n$. Each class contains only investors who are n^{th}-degree risk averse in the sense of Ekern (1980). All investors in $\mathbf{M}_2$ are second-degree risk averse, meaning they have increasing concave utility, and demand a premium to invest in a risky asset instead of a risk-free asset, as explained by Arrow (1965, 1971) and Pratt (1964).[2] Investors with higher degrees of risk aversion share common attitudes toward the location of risk in the distribution of

[1] See Derman and Miller (2016) for a broad discussion of option smiles and explanations thereof.

[2] In this paper we use words *positive, negative, increasing*, *decreasing* and *prefer* in the weak sense, and similarly for other terms of comparison. For example, x is positive if $x \geq 0$. Alternatively, we say *strictly positive* to mean $x > 0$.

returns, as described by Eeckhoudt and Schlesinger (2006), and Denuit and Eeckhoudt (2010). For examples, third-degree risk averters in $\mathbf{M}_3$ dislike risk in the left tail of the distribution, or alternatively said, they dislike downside risk (Menezes et al., 1980) and are *prudent* (Kimball, 1990), while fourth-degree risk averters in $\mathbf{M}_4$ dislike outside risk, which is risk in the extreme tails of a return distribution and are *temperate* (Kimball, 1993).[3]

Figures 1(a) and 1(b) provide examples of the bounds for call options with one week to expiration, displayed as IV profiles plotted against the ratio of strike price to underlying price (K/S_0). In-the-money (ITM) calls lie to the left, while out-of-the-money (OTM) calls are to the right. In each figure are: (i) three lower SD bounds, one for $n = 2, 3$ and 10, and (ii) one upper SD bound, which is identical across degrees n. The Black-Scholes (BS) annualized implied volatility, which is independent of the exercise prices of the options, is also plotted as a level line. The figures differ according to the distribution of the risky return underlying the calls. The distribution of log returns for Figure 1(a) is the symmetric Gaussian distribution, as in the BS model, while the distribution for Figure 1(b) is the aysmmetric skewed t distribution, intoduced by Hansen (1994). The two lower moments are identical across the figures and correspond to the historical values for the weekly SPX Index return over the period 1992 to 2022, while the third and fourth moments differ across the figures.[4] Importantly, Figure 1(b) recognizes that returns follow a negatively skewed and fat-tailed distribution as we find in our data, while Figure 1(a) does not.

Several significant features of stochastic dominance bounds are evident in the two figures, and these features demonstrate the interaction between investor attitudes and market risk. The range between the bounds declines as the index of risk aversion n increases in each of the two figures, while a large gap appears between the second and third degrees profiles. In fact the profiles of the $n = 3$ and 10 bounds nearly overlap, suggesting there is little need in this particular setting to study bounds beyond the third degree. Thus call option prices are likely to be higher in settings with only prudent investors and absent imprudent ones, and put-call parity leads to the same conclusion regarding put option prices. In other settings with more extreme kurtosis, the IV profile becomes more of a smile than a smirk, and some separation emerges between the third and higher-degree

[3] Investors in $\mathbf{M}_n \backslash \mathbf{M}_{n+1}$, $n \geq 2$, prefer (and are not averse to) n^{th}-degree risk. For examples, those in $\mathbf{M}_2 \backslash \mathbf{M}_3$ prefer downside over upside risk, while those in $\mathbf{M}_3 \backslash \mathbf{M}_4$ prefer risk in the extreme tails as opposed to the center of the distribution.

[4] Hansen's distribution and our estimation are discussed in Section 6 and Appendix D.

bounds on call options with longer tenors.

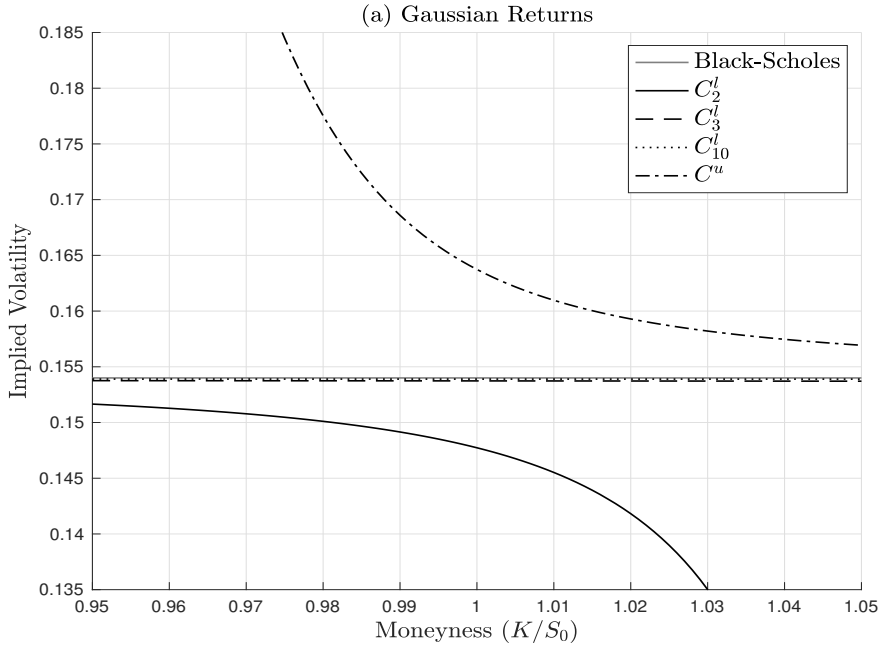
The BS implied volatility in Figure 1(a) lies between lower and upper bounds, and the series of lower bounds (as n rises) appears to approach it as a limit. Thus in the absence of asymmetry and excess kurtosis, and if options are priced by a representative agent with constant relative risk aversion as in Rubinstein (1986), the third or higher degree lower bounds tend be good estimates of the BS option price.

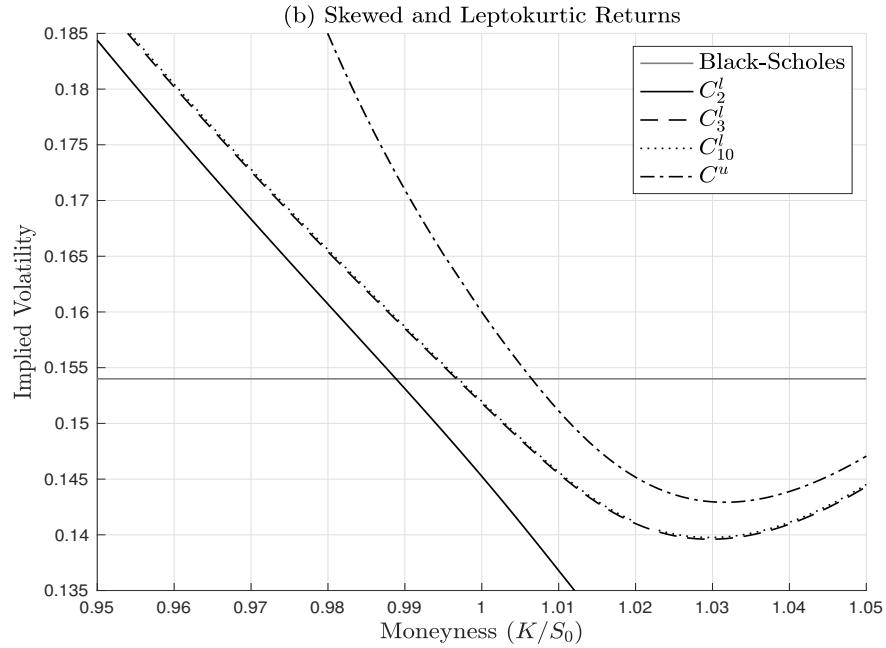
The bounds differ dramatically between the two figures. The IV profiles are level lines in the Gaussian environment, while a smirk or smile appears in the left-skewed and leptokurtotic environment. Both upper and lower bounds are mostly decreasing left to right in Figure 1(b), and except for the second degree bounds, they are bowl shaped in the right-hand region of OTM calls. Because the gap between the upper and lower bounds is relatively small for OTM calls, the figures suggest that an equilibrium profile will also exhibit a smirk when market participants dislike downside risk.

These figures suggest the overarching contributions of this paper. We introduce high-order stochastic dominance bounds, and use the bounds to describe the connections between investor attitudes and option prices. We demonstrate that an option value rises with risk in the underlying return within the region surrounding its exercise price, and we show this effect is most pronounced when investors are particularly averse to risk in that region. Again, prudent investors particularly dislike left-tail risk. This naturally leads to a smirk in the third-degree lower bound as seen in Figure 1(b), with IVs elevated in the left tail relative to the right tail. And if the risk in the left tail of the distribution of returns were to increase (with a skewness coefficient becoming increasingly negative, but a variance of return constant), this effect becomes more pronounced; the slope of the IV profile would increase in magnitude, becoming more negative. Alternatively, temperate investors dislike risk in the extreme tails of the distribution, and this leads to elevated IV levels in both left and right tails. If the tail risk were to increase (with kurtosis rising, while skewness and variance are constant), the tails of the IV profile increase. We construct a simple model of financial investment to demonstrate these ideas.

Figure 1
Bounds on Call Option Prices

Notes: Bounds are displayed as annualized implied volatilities (using the Black-Scholes model). The lower bounds apply to degrees of dominance $n = 2, 3$ and 10; a single upper bound applies to each degree n. The implied Black-Scholes volatility appears as a level line. The options are one week to expiration, the risk-free return is 2.5% per annum. In Figure 1(a) the distribution of the log return on the underlying shares is Gaussian, while in Figure 1(b) the distribution is the skewed Student's t distribution of Hansen (1994). The conditional moments of the underlying distributions are reported in Table 2.





1.1 Model Overview

We study a two-date economy in which investors hold optimal portfolios of risky shares and a risk-free bond as basis assets, without intermediate trading. If for given n all investors have n^{th}-degree risk aversion, the lower and upper bounds define a range of option prices that may exist in a two-sided zero-net-supply market. If an option is offered for sale at a price below the lower bound, our investors are willing buyers and none are sellers. Similarly, there are only sellers at a price above the upper bound.

Bounds are found by optimization, using the principle of strong duality. A primal problem for given n searches over investors, each represented as marginal utility $m \in \mathbf{M}_n$. The lower (or upper) bound is the minimum (or maximum, respectively) value the option, calculated as the discounted value of the future option payoffs, using the optimal m as a stochastic discount factor (SDF). Search requires an investor to hold an optimal portfolio of basis assets. The dual problem searches instead over portfolios of basis assets, namely values held in the risky shares and risk-free bond. In this case the lower bound represents the *dearest dominated portfolio*, which has the maximum value such that each investor in $\mathbf{M}_n$ prefers a marginal investment in the option over one in the portfolio. Analogously, the upper bound represents the *cheapest dominating portfolio*. Strong duality for either a lower or upper bound requires equality of the two optimal values, one primal and one dual.

Duality provides two alternative descriptions of the bounds, each with a distinct benefit. The dual problem allows a geometric interpretation of our optimization methods, while the primal identifies simple formulas to calculate or estimate the bounds in practice. A lower bound on a call option C_n^l on share with price S_0, for example, is the discounted expected option payoff,

$$C_n^l = E_F\left(\left(S_0 R - K\right)_+ m_n\left(R\right)\right). \tag{1}$$

Here, R_f and R are returns on the risk-free and underlying risky shares, with R following distribution F, and m_n is a piecewise polynomial function of R, simultaneously acting as a stochastic discount factor, and representing the marginal rate of substition (across time and states of the world) of a particular member of the class $\mathbf{M}_n$. A similar expression represents the upper bound. To calculate either bound one needs only: the particulars of the option; an estimate of F, the

risk-free return R_f, and the degree of dominance n. With these inputs, the theory identifies m_n as a function of the return R. Somewhat surprisingly, for a given physical distribution F and for all exercise prices K, m_n is the unique SDF for all lower bounds, and a second $m \in \mathbf{M}_n$ is the SDF for upper bounds.

We offer two interpretations of the bounds. Under the *market* interpretation all investors are members of a class $\mathbf{M}_n$, for some $n \geq 2$, and the bounds define ranges of option prices in a competitive financial market without arbitrage opportunities. The investors hold optimal portfolios of basis assets, and the model accords with classical analysis, including Ross (1976). A representative investor exists, and under this interpretation, an equilibrium price of an option falls between the upper and lower bounds.

Alternatively the *investor* interpretation describes the financial opportunities of individuals with n^{th} degree risk preferences, but who inhabit an economy that is not fully captured by the model. Some investors in the economy may not be members of $\mathbf{M}_n$, and in this case the model is similar to that of Almeida and Freire (AF, 2022) where price-setting investors may be heterogeous across option exercise prices. For example, we can imagine (but do not explicitly model) market makers who offer to buy from or sell options to investors, where the ask and bid prices may not fall between the bounds. The model then predicts that a target investor may increase welfare by an appropriately scaled purchase (sale) of an option at an ask (bid) price below a lower bound (above an upper bound, repectively). This logic can be used by individual investors and investment managers who consider options as a part of a portfolio of financial assets. If an investor is perceived to be prudent, for example, our third degree bounds are helpful in choosing the optimal portfolio.

Equation (1) calculates a lower SD bound as a discounted value of an option payoff using $m_n \in \mathbf{M}_n$ as a discount factor. In an alternative calculation the bound is the expected payoff under a corresponding risk-neutral distribution F_n, discounted at the risk-free rate:

$$C_n^l = \frac{1}{R_f} E_n \left((S_0 R - K)_+ \right). \tag{2}$$

We show that these distributions are ordered; for each $n \geq 2$, F_n second-degree stochastically dominates F_{n+1}. As a consequence, the lower SD bounds increase with degree n, $C_{n+1}^l \geq C_n^l$. More generally, this ordering implies the risk-neutral expectation of any convex function of R is

increasing with n. The Chicago Board Options Exchange VIX index provides an example. Carr and Madan (1998) derive VIX as the value of a portfolio of options written on the SPX. Because the portfolio weights are positive, the payoff is a convex function of R. Therefore, the market interpretation of our model predicts VIX is likely to be greater in an economy of uniformly prudent investors or temperate investors than in an economy with imprudent or intemperate investors, respectively.

1.2 Connections With Existing Literature

There are many outstanding models of stochastic dominance bounds for option prices. The seminal work is by Perrakis and Ryan (1984), Levy (1985) and Ritchken (1985). Like these authors, we consider two dates at which options trade in the absence of transaction costs. Alternatively, Constantinedes and Perrakis (2002) study European options trading in markets with frictions, while Constantinedes and Perrakis (2006) extends this theory to American options. Unlike our analysis, these theories rely solely on second-degree dominance. Perrakis (2019) reviews the literature on stochastic dominance and option prices, while Levy (2016) reviews applications of stochastic dominance more broadly.

Ritchken and Kuo (1989) and Mathur and Ritchken (1999) construct high-order SD bounds assuming the underlying asset return R follows a discrete distribution, and they calculate bounds by linear programming. In contrast, we assume R is continuously distributed on the interval $(0, \infty)$, and our bounds are found by search over stochastic discount factors (in our primal problems). Because we express bounds as moments of returns as in (1), economic interpretations of the bounds are easily provided.

Alternatives to SD bounds include the minimum-dispersion no-arbitrage bounds (MDNA) bounds of AF. These are found by search over investors in the HARA class, or equivalently by minimizing the distance between physical and risk-neutral distributions (using a Cressie-Read metric). Their marginal bound-setting investors are like ours in that they hold optimal portfolios of a risk-free bond and risky shares in a competitive and frictionless market, but unlike ours they are heterogenous across option exercise prices. Furthermore as AF recognize, the HARA investors that define MDNA lower bounds may prefer downside to upside risk, and these imprudent investors have utility functions defined on ranges of wealth that are bounded above. This contrasts with investors in

the classes $\mathbf{M}_n$, $n \geq 3$, all of whom are prudent, and contrasts with investors in $\mathbf{M}_2$, all of whom may have unlimited future portfolio returns. As a consequence our bounds are calculated directly when F is the Gaussian, Student t, or another distribution for logarithmic returns that covers the real line.

Bounds on assets' prices and risk premia have also been developed in competitive and incomplete markets by restricting SDFs indirectly. Bernardo and Ledoit (2000) place upper bounds on gain/loss ratios across all traded assets, while Cochrane and Saa-Requejo (2000) alternatively restrict assets' Sharpe ratios. Our model differs in that we constrain discount factors directly, confining them to a class $\mathbf{M}_n$ for each given order of risk attitudes n.

There is evidence of order flow from public investors as drivers of market index options. Bollen and Whaley (2004) demonstrate public buying pressure in the S&P Index put options leads to higher IV profiles of Index options. Garleanu et al. (2009) model demand pressure in option markets, and their empirical evidence shows that skew patterns in the IV profiles of SPX options increase with this pressure. Using similar data, Almeida and Freire (2023) calculate the monthly net buy orders of public investors for SPX options, and use these data to explain 30-day option returns. While unconditional average returns are negative, the returns are positive for both calls and puts in periods when public investors are net buyers of the respective options.

These authors recognize options are non-redundent securities traded in zero-net-supply markets, participants of option markets are heterogeneous, and inventories of the market makers cannot be perfectly hedged. Market makers are sometimes the marginal investors pricing options. For these reasons, option prices and IV profiles will deviate from the predictions of classical models of equilibria and models of SD bounds, including the market interpretation of our model. This leads us to the investor interpretation noted above. Prudent or temperate investors may use our bounds as benchmarks for identifying favorably-priced options for their portfolios.

The remainder of the paper proceeds as follows. Section 2 introduces the model structure and the problem faced by investors. It provides a formal introduction of risk attitudes and the classes $\mathbf{M}_n$. Section 3 describes in general terms the dual and primal problems that define the bounds, while Section 4 presents our methods of solution to those problems. Our main results regarding upper and lower bounds are in Section 5, and numerical examples are in Section 6. Section 7 concludes, and Appendices follow.

2 Market Structure and Risk-Averse Investors

We study a financial market with investors trading shares of basis assets: risky shares and a risk-free bond. Investors trade shares now (time 0) at the price $S_0 > 0$, giving future (time T) payoff S_T and random return $R = S_T/S_0$, and they believe R follows a continuous and strictly increasing cumulative distribution $F : (0, \infty) \to \mathbb{R}$, with

$$\lim_{r \to 0} F(r) = 0 \text{ and } \lim_{r \to \infty} F(r) = 1,$$

and a finite and positive expected return $0 < E_F(R) < \infty$. This distribution is either an objective or subjective belief, depending upon the interpretation of the model. If we choose our model to represent a competitive economy of rational investors with homogeneous beliefs, F is objective. If instead our investors inhabit an economy that is not fully captured by our model, F is their subjective belief. In either case, our bounds are appropriate for all investoprs in a class $\mathbf{M}_n$.

The bond trades now at a unit price of \$1 and offers the return R_f such that the risk premium on the shares is positive $E_F(R) - R_f > 0$. Call and put option contracts are written on the shares, and these have future payoffs $c(r) = (r - K)_+$ and $p(r) = (K - r)_+$, respectively for returns $r \in (0, \infty)$, where K is the exercise price, $0 \leq K < \infty$.[5] The call options give the investor the right but not the obligation to buy shares at their respective exercise prices at time T, while puts are rights to sell shares. The option payoffs and exercise prices are in units per dollar invested in the share, and bounds on current prices are reported similarly. (A conversion to commonly-reported per-share units appears later.)

2.1 Investors' Portfolios

Risk-averse investors trade to maximize expected utility of consumptions at dates 0 and T. Setting aside the option contracts for the moment, an investor with wealth w_0 holds a portfolio of the bond and risky shares, choosing savings s and investment α to solve

$$\max_{s>0, \alpha \geq 0} E_F\left(u\left(w_0 - s, s\left(\alpha\left(R - R_f\right) + R_f\right)\right)\right), \tag{3}$$

[5] Despite that an option's payoff, value and price depend on the exercise price K, we simplify notation by writing these values without explicit dependence.

where utility function u is increasing and concave, and it is at least once differentiable in its arguments. The first-order conditions

$$1 = R_f E_F\left(m\left(R\right)\right) \tag{4}$$

$$0 = E_F\left(\left(R - R_f\right) m\left(R\right)\right), \tag{5}$$

identify optimal savings and investment, where

$$m\left(r\right) = \frac{\partial u\left(x,y\right)/\partial y}{\partial u\left(x,y\right)/\partial x}, \tag{6}$$

evaluated at $x = w_0 - s$, $y = s\left(\alpha\left(r - R_f\right) + R_f\right)$ and $r \in (0, \infty)$. We assume investors initially hold portfolios of the basis assets that satisfy these two conditions.[6]

An investor's marginal willingness to buy or sell an option establishes bounds on the option's price. For a concrete example consider a call option on the risky shares, and suppose one investor with marginal utility m considers trading at a price C. The sign of difference between marginal value and cost,

$$E_F\left(c\left(R\right) m\left(R\right)\right) - C, \tag{7}$$

indicates the desire of that investor or any investor with marginal utility m to trade. If the difference is positive or negative, the investor willingly buys or sells the call, respectively, while zero represents indifference. Because options trade in two-sided (and zero-net-supply) markets, an equilibrium C lies in a range such that either: some investors are willing buyers while others are sellers of the option, or all investors are indifferent. If C is too low and all investors are willing buyers, then none are willing sellers, indicating a one-sided market. Similarly C cannot be too high. The lower and upper bounds define the range of prices that are consistent with two-sided markets. We study these bounds as they vary with investors' attitudes toward risk.

[6]This specification does not require time-additive expected utility. We require positive savings, $s > 0$; a sufficient condition for this result is $\partial u\left(x,y\right)/\partial x < \lim_{y \downarrow 0} \partial u\left(x,y\right)/\partial y \times R_f$. Because $E\left(R\right) > R_f$, each investor's position in the shares is strictly positive, $\alpha > 0$ implying that $m\left(r\right)$ is decreasing with r. See Arrow (1970) for discussion.

2.2 Investors' Attitudes Toward Risk

Investors' current marginal values of the option $E_F(c(R)m(R))$ may be heterogeneous for a variety of reasons, including differences in their information or their desire to smooth consumption across time. However we focus solely on differences in their attitudes toward risk, and nested classes $\mathbf{M}_n$, $\mathbf{M}_{n+1} \subset \mathbf{M}_n$, $n \geq 2$, capture these differences. All investors are in $\mathbf{M}_2$ and are risk averse, demanding a premium $E(R) - R_f > 0$ to hold the shares. Investors in $\mathbf{M}_3$ differ from other members of $\mathbf{M}_2$ in that they dislike third-order risk, while investors in $\mathbf{M}_4$ dislike fourth-order risk. Generally, investors in $\mathbf{M}_n$ differ from those in $\mathbf{M}_{n-1}$, $n \geq 2$, in that they dislike n^{th}-order risk. Holding constant the first $n-1$ moments, n^{th}-order investors prefer either higher or lower values of the n^{th} moment of distribution F, depending on whether n is odd or even. For examples, third-order investors prefer gambles with positive skewness and are averse to negative skewness, while fourth-order investors prefer lower to higher kurtosis, again holding lower moments constant.

We rely on the *multiply monotone functions* of Williamson (1956) to create classes $\mathbf{M}_n$.

Definition 1: A function $f : (0, \infty) \to \mathbb{R}$ is p-times monotone where p is an integer, $p \geq 2$, if $(-1)^k f^k(t)$ is positive, decreasing and convex for $t > 0$ and $k = 0, 1, 2, ..., p-2$.[7] *When $p = 1$, f is simply positive and decreasing.*

Formally we have

Definition 2: $\mathbf{M}_n$ is the class of investors with' marginal utility functions $m : (0, \infty) \to \mathbb{R}$ that are $(n-1)$-times monotone.

Each $m \in \mathbf{M}_2$ is positive and decreasing (one-time monotone), and each investor is averse to mean-zero gambles. If in addition $m \in \mathbf{M}_n$, $n > 2$, derivatives $m^{(k)}$, $k = 0, ..., n-3$, exist with $(-1)^k m^{(k)}$ positive, decreasing and convex; these investors are averse to each k^{th} order risk, $k = 2, ..., n$. This representation of investors is similar to prior work in which risk preferences appear as signed high-order derivatives of utility. One example is Ekern (1980), who defines stochastic dominance for integer orders $n \geq 2$; his investors are n^{th}-degree risk averse if utility is increasing and concave, with derivatives alternating in sign up to order n.[8] Other examples are:

[7] For $k = 0, 1, ...$ and function f, $f^{(k)}$ is the k^{th} derivative.

[8] We apply Williamson's characterization to marginal utility m, and not directly to the utility function u. As a consequence, u is differentiable up to order $n-2$ with $(-1)^{n-2} u^{(n-2)}$ required to increasing and concave.

(i) Denuit and Eeckhoudt (2010), who would say the utility functions corresponding to $m \in \mathbf{M}_n$ are *n-increasing concave functions,* and (ii) Caballe and Pomansky (1999), who study the case of *mixed risk aversion* in which $n = \infty$.[9]

Informally we refer to members of $\mathbf{M}_n$ in various ways. Alternatively we write: *m is an* n^{th}*-degree risk averse investor*, or *an investor is in* $\mathbf{M}_n$*,* or *m is in* $\mathbf{M}_n$, or $m \in \mathbf{M}_n$, $n \geq 2$, to mean that the investor's marginal utility m is $(n-1)$-times monotone. We refer to m as either an investor or a discount factor, recognizing that m represents each of these concepts.

3 The Economics of SD Bounds on Option Prices

Bounds on option prices are found by search over investors with common risk attitudes within a class $\mathbf{M}_n$. Bounds are alternatively found by search over portfolios of the basis assets. The optimality of the two solutions is demonstrated via the principle of strong duality. For any option and for each of the upper and lower bounds, candidate solutions for the primal and dual are shown to be equivalent. This demonstrates optimality.

3.1 Primal Problems - Search Over Investors

Consider the lower SD bound on a call option. It is the objective of the primal problem,

$$C^p \overset{def}{=} \min_{m \in \mathbf{M}_n} E_F \left(c\left(R\right) m\left(R\right) \right), \tag{8}$$

subject to the equalities (4) and (5) as constraints. C^p is the minimum value of the option's payoffs using the marginal utility m of a particular investor as the discount factor, found by search over investors holding only basis assets in their optimal portfolio, as in problem (3). As a consequence the factor m that achieves the minimum in (8) also equates the discounted value of a return to the cost of a return (one dollar) for each basis asset.

Problem (8) represents a search over two-sided option markets. To explain this idea consider the marginal changes in investor welfare when options are bought or sold. If a unique investor (or a collection of homogenous investors) with marginal utility m^p is the solution to (8) then m^p is a discount factor that delivers the objective value C^p, and the investor is indifferent to buying or

[9] Trautmann and Kuilen (2018) review studies of high-order risk preferences.

selling the option at a market price of C^p. All other investors in $\mathbf{M}_n$ who satisfy the constraints are willing buyers at this price, and these investors assess a value for the option above C^p; otherwise, m^p is not the solution. If a broker opened trade in the option at a price above C^p, some of these investors, including investor m^p would instead be willing sellers, leading to a two-sided market. Alternatively if trade is offered at a price C^p, the option n^{th}-degree dominates each and every possible portfolio of the basis assets, and no investor in $\mathbf{M}_n$ is a willing seller of the option. Thus problem (8) seeks the lowest price within two-sided markets.

An upper bound on the call option price is explained similarly. It too is the outcome of a search within two-sided markets, but it is the supremum of the objective in (8), again subject to (4) and (5). No active market in the option exists at prices above the bound because the option is dominated by a portfolio of basis assets, and no investor is willing to buy the option. The upper and lower bounds on put options are obtained later from those on call options, using put-call parity.

3.2 Dual Problems - Search Over Portfolios

While primal problems search over investors, the respective dual problems search over portfolios of underlying basis assets. Furthermore, whereas the primals search within two-sided markets, the duals search within one-sided markets. The dual to (8) is an example:

$$C^d \overset{def}{=} \max_{v_1,v_2} v_1 + v_2 \tag{9}$$

subject to

$$E_F\left(c\left(R\right)m\left(R\right)\right) \geq v_1 E_F\left(Rm\left(R\right)\right) + v_2 R_f E_F\left(m\left(R\right)\right), m \in \mathbf{M}_n. \tag{10}$$

This problem seeks the portfolio v_1, v_2 with maximum value C^d, where v_1 and v_2 are dollar values invested in the shares and the bond, respectively. Search is limited to portfolios for which the personal value of the option (on the left of the inequality (10)) is no less than the value of the portfolio (on the right) for each and every investor in $\mathbf{M}_n$. Inequality (10) is a dominance requirement, restricting us to search over portfolios that are dominated by the option. If the option is offered for sale at a price below C^d, every investor in $\mathbf{M}_n$ is a willing buyer and no one is a willing seller. Thus C^d is the largest possible asking price in these buyers-only markets, and the solution to the

dual is the *dearest dominated portfolio* v_1, v_2.

3.3 Strong Duality

The primal objective for a lower bound is no less than that of the dual, meaning $C^p \geq C^d$. For any $m \in \mathbf{M}_n$ satisfying the constraints of the primal, and any v_1, v_2 satisfying those of the dual

$$\begin{aligned} E_F\left(c\left(r\right)m\left(r\right)\right) \geq & v_1 E_F\left(Rm\left(R\right)\right) + v_2 R_f E_F\left(m\left(R\right)\right) \\ = & v_1 + v_2. \end{aligned} \tag{11}$$

Therefore optimality is identified by an investor and a portfolio that satisfy (11) as an equality. In this case $C^p = C^d$ and the lower bound on the call option price is given equivalently as the value of either the primal or the dual objective. In particular the lower SD bound is equivalent to the cost of the dearest dominated portfolio of basis assets.

In the case of the upper bound, a minimal portfolio value is found in the dual, and the inequalities (10) and (11) are reversed. The dual problem identifies the *cheapest dominating portfolio*, and strong duality says the upper SD bound is the cost of this portfolio.

4 A Generating Class of Investors

The prior discussion presents a theoretically sound but practically infeasible direction to obtain bounds on option prices. A direct attack on the problem requires search over the infinite-dimensional space of marginal-utility functions $\mathbf{M}_n$, $n \geq 2$ in the primal problem (8), and similarly in the dual (9) there is one constraint for each member of $\mathbf{M}_n$. To simply matters we introduce for each $n \geq 2$ a generating subclass of investors $\mathbf{G}_n$, and by substitution of variables we develop a useful method to solve both the primal and dual problems. The discount factors defining stochastic dominance bounds on option prices are scaled members of this subclass:

$$\mathbf{G}_n = \left\{\mathbf{1}, \left\{m_{n,g} : g \geq 0\right\}\right\}, \tag{12}$$

where

$$m_{n,g}\left(r\right) = \left(g - r\right)_+^{n-2}, \ r \in \left(0, \infty\right). \tag{13}$$

Our solutions to both primal and dual problems are based on members of $\mathbf{G}_n$.

Each member of $\mathbf{G}_n$ has marginal utility that is either the constant one, representing a risk-neutral investor, or a positive and decreasing function indexed by $g \in (0, \infty)$, representing a risk-averse investor. Thus each member of $\mathbf{G}_n$ is also in $\mathbf{M}_n$, and unlike $\mathbf{M}_n$, $\mathbf{G}_n$ is a collection of parametric functions. In addition $\mathbf{G}_n$ generates $\mathbf{M}_n$ in the sense that each $m \in \mathbf{M}_n$ is equivalent to a linear transformation of the members of $\mathbf{G}_n$. Relying on the work of Williamson (1956) we prove in the appendix

Theorem 1. For each class $\mathbf{M}_n$, $n \geq 2$, *the marginal utility of an investor* $m \in \mathbf{M}_n$ *satisfies*

$$m(r) = \overline{m} \times \mathbf{1} + \int_{g=0}^{\infty} m_{n,g}(r)\, dy(g), \; r \in (0, \infty), \tag{14}$$

with $\overline{m} \geq 0$ *and* $y \in \mathbf{M}_1$, *where* $\mathbf{M}_1$ *is the class of increasing functions on* $(0, \infty)$, *and any* $(n-1)$*-times monotone marginal utility* m *is obtained from (14) by choosing the appropriate* $\overline{m}$ *and* y.

Roughly speaking, the marginal utility of any n^{th}-degree risk-averse investor is equivalent to a weighted sum of the parametric marginal utilities in $\mathbf{G}_n$. Positive weights are used in (14); the weights on the $m_{n,g}$ are defined by the increments of the increasing function y.[10] This result simplifies our search problems; it allows us to substitute for m in both primal and dual using parametric functions. In the end, SD bounds on option prices are discounted option payoffs in which elements of $\mathbf{G}_n$ define the discount factor.

4.1 Members of $\mathbf{G}_n$

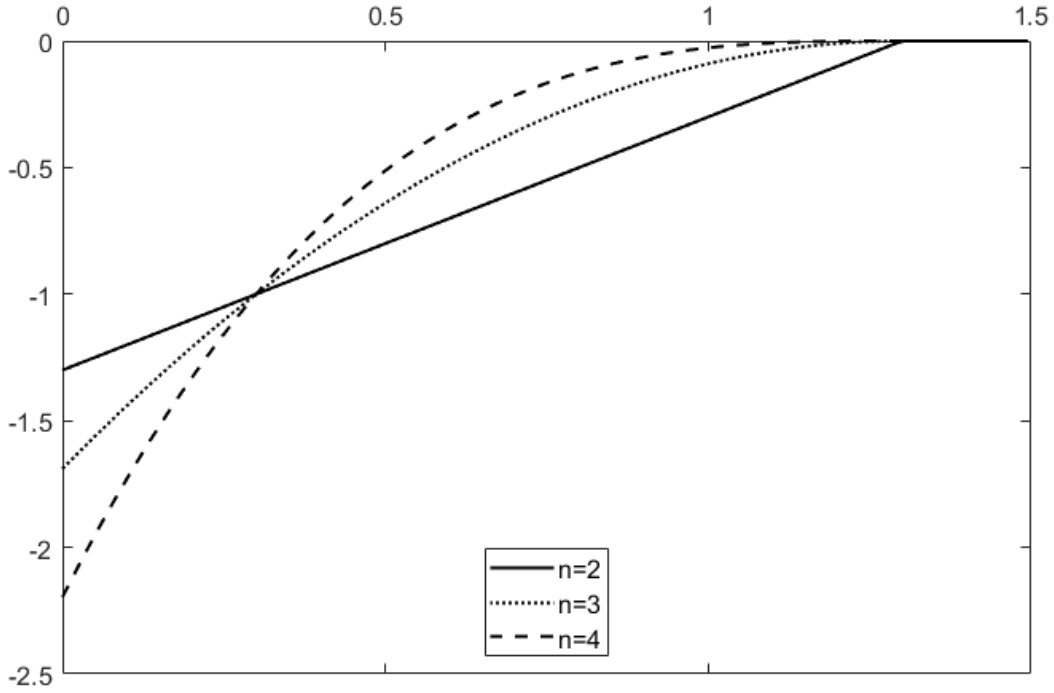
A member of $\mathbf{G}_n$ has marginal utility that is either the constant one, or a positive decreasing function $m_{n,g}$ indexed by $g \in (0, \infty)$. The utility corresponding to any $m_{n,g}$, say, $U_{n,g}$ exhibits standard features. Figure 2 plots the $U_{n,g}$ for $n = 2$ to 4 and $g = 1.3$ on the interval $(0, 2]$. They appear as piecewise polynomials with g as a knot, separating the utility into regions to the left and

[10] The integral $\int_{g=0}^{\infty} m_{n,g}(r)\, dy(g)$ tends to zero as r increases without bound (because the limiting value of each $m_{n,g}$ is zero) so that $m(r) \underset{r \to \infty}{\to} \overline{m}$. Riemann-Stieltjes integration is used, recognizing that function y may have countable number of discrete jumps. In particular, the integral in (14) picks off a single member of $\mathbf{G}_n$ when y jumps discretely at $g = g^*$ and is constant on each side of g^*. For example if $\overline{m} = 0$, $y = -a$ for $g < g^*$ and $y = 0$ for $g \geq g^*$ then $m(r) = a m_{n,g^*}(r)$.

right. On $(0, g)$: (i) $U_{n,g}$ is strictly increasing; (ii) for $n = 3, 4$, it is strictly concave; and (iii) for $n = 4$, $U_{n,g}$ is strictly decreasingly concave in the sense that the third derivative is positive. On the interval $[g, \infty)$, each function is zero. Globally on $(0, \infty)$ each $U_{n,g}$ is increasing and concave.[11]

Figure 2
Utility Functions $U_{n,g}$

Notes: This figure plots the utility functions $U_{n,g}$ for $n = 2, 3$ and 4 and a select value of $g = 1.3$.



4.2 Power Utility As An Example

Power utility provides an example in which the equality (14) holds for all $n \geq 2$. In this case $u(r) = \frac{(A+r)^{1-B}-1}{1-B}$, $A \geq 0$ $B \geq 0$, and $r \geq 0$, and equality (14) is

$$(A + r)^{-B} = \int_{g=r}^{\infty} (g - r)^{n-2} \, dy(g), \tag{15}$$

[11] Admittedly the utility functions $U_{n,g}(r)$ exhibit *bliss*; marginal utility is zero for returns r greater than g. However, this is not a troubling issue for SD option bounds in cases of third- or higher degrees of dominance; see the discussion of Theorem 2 below.

with $\overline{m} = 0$. If $n = 2$ then $y(r) = -(A+r)^{-B}$ solves (15), while for each $n \geq 3$ we differentiate $n-2$ times with respect to r on each side of (15) and after integrating we obtain

$$y(r) = -\mathbb{B}_n (A+r)^{-B+2-n}, \ r \in (0,\infty),$$

where $\mathbb{B}_n = \frac{\Pi_{j=1}^{n-2}(B+j-1)}{(n-2)!} > 0$. Thus y is an increasing function.

4.3 Stochastic Dominance

The use of generating subclasses of investors facilitates general comparisons of stochastic dominance. In the finance literature dominance of one random return or payoff over another is defined by the unanimity of choice within a class of investors.[12] We say of our setting: *Portfolio return* R^* *n^{th}-degree dominates* R_* *if all members of the class* $\mathbf{M}_n$ *prefer* R^* *to* R_*. Theorem 1 implies that we may use $\mathbf{G}_n$ as a stand-in or substitute for $\mathbf{M}_n$. Because $\mathbf{G}_n \subset \mathbf{M}_n$, every investor in $\mathbf{G}_n$ prefers R^* over R_* when R^* dominates R_*. However because the weights in (14) are positive, the converse also holds. We have

Corollary 1. The return R^* *n^{th}-degree dominates the return* R_* *if and only if each member of the class* $\mathbf{G}_n$ *prefers* R^* *over* R_*, *meaning* $E_F(R^*) \geq E_F(R_*)$ *and*

$$E_F(U_{n,g}(R^*)) \geq E_F(U_{n,g}(R_*)) \ \textit{for all} \ g \in (0,\infty).$$

This result encourages us to search over $\mathbf{G}_n$ instead of search over $\mathbf{M}_n$ to find SD bounds on option prices. Unanimity of preference among investors in $\mathbf{G}_n$ is sufficient to say there is unanimity among members of $\mathbf{M}_n$ as well.[13]

[12] See Perrakis (2019) for a detailed discussion of dominance in the finance literature, and see his referenced articles for examples and applications.

[13] The conclusion of Corollary 1 is similar to but distinctly different from the Mean-Lower-Partial-Moment rules of Bawa (1975). Bawa's rules apply to degrees of dominance up to third degree, while our conclusions apply to all degrees $n \geq 2$. Also our methods of deduction differ; we first establish the generating classes $\mathbf{G}_n$, while Bawa studies only comparisons of dominance.

5 Stochastic Dominance Bounds for Option Prices

The optimization problems (8) and (9) are solved after substitution for m using Theorem 1. The appendix shows how this is done. New choice variables appear, which are the constant $\overline{m}$ and the function y in equality (14). Because the revised problems rely on class $\mathbf{G}_n$, and only indirectly on $\mathbf{M}_n$, the values of options, risky shares and bonds are expressed as moments of payoffs with parametric discount factors. Perhaps surprisingly, a single constant discount factor $\overline{m} = 1/E_F(R)$ defines all upper bounds on options (across exercise prices and degrees n), while a second, positive and decreasing marginal utility $m_{n,g}$ defines all lower bounds (across exercise prices). The identification of the appropriate $g \in (0, \infty)$ for each n is a key step in demonstrating the lower bounds.

5.1 Lower Bounds on Call Option Prices

The value of a call option to an investor $m_{n,g} \in \mathbf{G}_n$ is

$$\begin{aligned} C_n(g) &\overset{def}{=} E_F\left(c(R)\, m_{n,g}(R)\right) \\ &= \int_{r=0}^{\infty} (r-K)_+ (g-r)_+^{n-2}\, dF(r), \end{aligned} \tag{16}$$

while the moments $I_n(g)$, $R_n(g)$ and $P_n(g)$ that appear below are defined similarly.[14] Each of these represents the marginal value of an additional unit of an asset to an investor holding only a single risky share. Lower bounds are ratios of these moments, and together they require four inputs: the risk-free return R_f, degree of dominance n, distribution of the risky return F, and the index g identifying an investor in $\mathbf{G}_n$ with discount factor $m_{n,g}$.

In the appendix we prove

Theorem 2 - Lower Bound for a Call Price. For each exercise price K and degree of dominance $n \geq 2$, the price of a call option is no less than

$$C_n^l = \frac{C_n(g_n)}{I_n(g_n)\, R_f}, \tag{17}$$

[14] We set $I_n(g) = E_F(m_{n,g}(R))$, $R_n(g) = E_F(R m_{n,g}(R))$ and $P_n(g) = E_F(p(R)\, m_{n,g}(R))$. Hence $I_n(g)$ is the value of a bond with a \$1 payoff (not R_f), while $R_n(g)$ and $P_n(g)$ are values of the share and put using $m_{n,g}$ as a discount factor. As noted above, we write option payoffs, prices and values without explicit identification of the exercise price.

where g_n is the root of

$$0 = R_n(g) - I_n(g) R_f = E_F\left((R - R_f) m_{n,g}(R)\right). \tag{18}$$

This bound satisfies strong duality. The minimum in the primal (8) is C_n^l when

$$\overline{m} = 0 \text{ and } y(g) = \begin{cases} 0 \text{ if } g \geq g_n \\ \frac{-1}{R_f I_n(g_n)} \text{ if } g < g_n \end{cases}, \tag{19}$$

and the maximum in the dual (9) is C_n^l when the portfolio is

$$v_1 = \begin{cases} 0 \text{ if } g_n \leq K \\ \left(\frac{d}{dg} \frac{C_n(g)}{I_n(g)} \Big/ \frac{d}{dg} \frac{R_n(g)}{I_n(g)} \right)_{g=g_n} \text{ otherwise} \end{cases} \tag{20}$$

$$v_2 = C_n^l - v_1. \tag{21}$$

Discussion. The critical value g_n identifies the unique investor $m_{n,g} \in \mathbf{G}_n$ who holds an optimal portfolio of a single risky share and nothing of the bond. It is the root of equality (18), which in turn is equivalent to the the first-order condition (5) of the primal problem (8), after the substitution for m using Theorem 1. Investors in the generating class with g smaller or larger than g_n want to be long or short the bond, respectively, in their portfolios.

The lower bound (17) is equivalently written

$$C_n^l = E_F\left((R - K)_+ m_n(R)\right) \tag{22}$$

where

$$m_n(R) \overset{def}{=} \frac{m_{n,g_n}(R)}{R_f I_n(g_n)}, \tag{23}$$

with the factor $\frac{1}{R_f I_n(g_n)}$ chosen so that m_n satisfies the first-order condition (4). Equation (22) represents a simple method-of-moments estimator of the lower bound when a sample distribution substitutes for F. Because the ratio $R_n(g) / I_n(g)$ is strictly increasing in g, the critical value g_n is easily estimated as the root of (18).

If $n = 2$ we obtain Ritchken's second-degree lower bound. This is the conditional expected call

payoff discounted at the risk-free rate: $C_2^l = \frac{1}{R_f} E_F\left((R-K)_+ | R \leq g_2\right)$.[15] For all exercise prices $K \geq g_2$, $C_2^l = 0$, and the analogous result holds for all $n \geq 2$,

$$C_n^l = 0 \text{ if } K \geq g_n.$$

This limits the usefulness of second-degree bounds for far-out-of-the-money calls (and in-the-money puts), but this is not a troublesome issue for $n > 2$; g_n increases with n (see Lemma 3 in the appendix, and Figures 1(a) and 1(b)), and numerical analysis shows g_3 is much larger than g_2. Thus, there is considerable advantage to using third- over second-degree stochastic dominance bounds, provided one believes investors are financially prudent.

The lower bound is alternatively interpreted as the equilibrium value of the option in a risk-neutral economy. For given n consider the distribution

$$F_n(r) = \frac{1}{E_F(m_n(R))} \int_{x=0}^{r} m_n(x)\, dF(x), \; r \in (0,\infty), \tag{24}$$

and the associated expectations operator E_n. This is a proper distribution on $(0,\infty)$; it is increasing, $F_n(0) = 0$ and $F_n(r) = 1$ for $r \geq g_n$.[16] The risk-free return solves

$$1 = R_f E_F(m_n(R)) \tag{25}$$

while the share return satisfies

$$1 = E_F(R m_n(R)) = \frac{1}{R_f} E_n(R) = \frac{1}{R_f} \frac{R_n(g_n)}{I_n(g_n)}. \tag{26}$$

These equalities are the constraints (4) and (5). The second result also is a risk-neutral valuation of a risky share using the distribution F_n; the expected share return under F_n is R_f. Similarly,

[15] Compare equation (17) to Ritchken's equation (28), substituting g_n for his s_j^*, and compare our equation (18) to his equality (29). For $n = 2$, $F_2(r) = F(r|R \leq g_2)$.

[16] F_n is not strictly increasing.

the price of a call option in the economy is

$$\begin{aligned} \frac{1}{R_f} E_n\left((R-K)_+\right) &= E_F\left((R-K)_+ m_n(R)\right) \\ &= C_n^l. \end{aligned} \tag{27}$$

Thus the risk-neutral price under distribution F_n is the equilibrium price of the option in an economy with the representative investor's marginal utility m_n and utility level U_{n,g_n}. It also in the lower bound on the call price in the absence of the representative investor.

In summary, the lower bound C_n^l is found by two equivalent and standard calculations. One is to discount using the factor m_n of an investor who represents the bound. The second is the expected payoff under the risk neutral distribution F_n, discounted at the risk-free rate.

The solution v_1, v_1 to the dual satisifies two important conditions. First, the portfolio value $v_1 + v_2$ is equal to the lower bound C_n^l, which in turn is the value of the primal objective (8). This is the equivalence of strong duality. Second, the individual positions v_1 and v_1 in (20) and (21), respectively, satisfy the constraints. The proof of Theorem 2 demonstates (10) holds as an equality at $m = m_{n,g_n}$ and otherwise holds as an inequality, when evaluated at the portfolio in (20) and (21).

Numerical analysis shows dual portfolios generally are highly levered with $v_1 >> 1$ and $v_2 << 0$. However our analysis sets R_f equal to the promised return on a short-term Treasury security, as is common in the financial literature. It might appear that the bound C_n^l decreases as R_f increases (note R_f in the denominator of 17), but C_n^l increases with R_f, and this is because g_n increases as well. These facts suggest for applied work that C_n^l be calculated by setting R_f equal to a short-term non-governmental borrowing rate such as SOFR or the prime rate of interest. Lower bounds calculated with R_f set to the Treasury rate are unnecessarily conservative.

If we apply our bounds to complete markets, and if we price all assets price using the marginal utility (23) as a SDF, then there is arbitrage. Because $m_n = 0$ on the interval (g_n, ∞), the price of a call option with a sufficiently high exercise price is costless, for example. This feature is not shared by the theories of either Bernardo and Ledoit (2000), who proscribe high gain/loss ratios, or Cochrane and Saa-Requejo (2000), who proscribe high Sharpe ratios, but it is shared by all degrees of stochastic dominance bounds, including the oft-used second-degree dominance..

Because arbitrage is viewed as a bug in financial theory, we should consider two points.

First, the range of returns in which $m_n = 0$ varies with degree of dominance n. This range in the right tail has relatively low probability, and the associated probability of return becomes miniscule and insignificant as the degree of dominance n increases. Consider as examples the likelihoods for degrees $n = 2$, 3, 4, and 10 from our numerical work:

Table 1
The Values g_n and Associated Tail Probabilities Across Tenors

Notes: Values g_n, as determined by equation (18), across different option tenors T. The moments of the underlying risky asset distribution are in Table 2, and the risk-free rate is 2.5% per annum. The tail probabilities, $\Pr_F(R \geq g_n)$, are shown in parentheses.

$T \setminus n$	2	3	4	10
1/52	1.042	1.464	1.931	4.736
	(0.0197)	(4.76×10^{-12})	(7.353×10^{-15})	(2.76×10^{-19})
1/12	1.066	1.447	1.901	4.643
	(0.0520)	(4.87×10^{-7})	(8.68×10^{-9})	(1.72×10^{-11})
3/12	1.103	1.495	2.000	5.079
	(0.106)	(8.51×10^{-6})	(2.02×10^{-7})	(8.10×10^{-10})
6/12	1.145	1.518	2.032	5.202
	(0.158)	(4.34×10^{-5})	(8.06×10^{-7})	(2.60×10^{-9})
1	1.212	1.571	2.088	5.331
	(0.218)	(6.58×10^{-4})	(9.71×10^{-6})	(1.71×10^{-8})

These probabilities are calculated using our baseline parameter estimates for weekly SPX returns (described in detail later), and they are tiny for $n \geq 3$. This is consistent with the fact that in practice, options with exercise prices in the ranges (g_n, ∞) are unlikely to to be traded. Investors have little interest in these options given that the chance of a positive payoff is almost immeasureable. This suggests that the theoretical existence of arbitrage is unlikely to be a bug in applied work.

Second, we may interpret C_n^l as an approximation of the lower bound in the absence of arbitrage. The SDF m_n is a scaled version of m_{n,g_n}, and each $m_{n,g}$ can be increasingly well approximated by a series of positive marginal utilities. For example if $\overline{m} > 0$, the SDF $\frac{m_{n,g_n}(r)+\overline{m}}{R_f I_n(g_n)}$ is uniformly positive on $(0, \infty)$, and there is pointwise convergence of the series:

$$\frac{m_{n,g_n}(r) + \overline{m}}{R_f I_n(g_n)} \underset{\overline{m}\to 0}{\longrightarrow} m_n(r), \text{ for all } r \in (0, \infty).$$

Thus a lower bound on an option price C_n^l in (22) approximates the discounted payoff calculated using a positive SDF.

5.2 Lower Bounds on Put Option Prices

The lower bound on a European put option is found via put-call parity. Following Merton's no-arbitrage argument, the equality of payoffs

$$p(R) = c(R) - R + K$$

holds for put and call options. Applying a discount factor $m_n \in \mathbf{G}_n$ as a linear operator, the lower bound on the put price is

$$P_n^l = C_n^l - 1 + K/R_f = E_F\left((K-R)_+ m_n(R)\right) = \frac{1}{R_f} E_n\left((K-R)_+\right).$$

5.3 Lower Bounds Increase With Degree of Dominance n

For a given physical distribution F of the risky share return, the risk-neutral distributions F_n defined in (24) have equal means. For every $n \geq 2$, $E_n(R) = R_f$. At the same time, the distributions are inversely ordered by risk (see Rothschild and Stiglitz (RS, 1969)) as n increases. Specifically, distribution F_{n+1} has greater risk than F_n, $n \geq 2$. These facts imply the lower SD bounds on call and put option prices increase with the degree of dominance n.

Theorem 3 - Degrees of Dominance and Lower Bounds. We have

$$C_n^l \leq C_{n+1}^l \text{ and } P_n^l \leq P_{n+1}^l, \text{ for all } n \geq 2.$$

Given equal means and greater dispersion of returns, RS would say *distribution F_{n+1} has greater weight in the tails than F_n*. This idea together with the fact that the call and put payoffs are convex functions provides an understanding of the theorem. The expected values of convex functions, including $E_n(c(R)) = E_n\left((r-K)_+\right)$ and $E_n(p(R)) = E_n\left((K-r)_+\right)$ rise as the likelihood of returns in the tails of the distributions F_n grows larger.[17]

[17] An example of greater risk of F_{n+1} over F_n is in Appendix B.

5.4 Upper Bounds for Call and Put Prices

We prove in the appendix:

Theorem 4 - Upper Bound for a Call Price. For each $n \geq 2$, the upper bound on the call price is

$$C_n^u = C^u \stackrel{def}{=} \frac{E\left(c\left(R\right)\right)}{E\left(R\right)}, \tag{28}$$

Strong duality holds: the values of the objectives in the revised primal (B.4) and dual (B.7) (in the appendix) are each C^u. The optimal portfolio in the dual problem is

$$v_1 = \frac{E\left(c\left(R\right)\right)}{E\left(R\right)}, \text{ and } v_2 = 0. \tag{29}$$

Discussion. The upper bound (28) for all $n \geq 2$ is the expected call payoff discounted by the expected return on the share, and it is the upper bound found by Ritchken for second degree dominance using a discrete distribution F. It is equivalent to the value of the option for a *risk-neutral investor who holds only the share* and has marginal utility

$$m_{RN}\left(r\right) = \frac{1}{E\left(R\right)}, \;\; r \in \left(0, \infty\right).$$

A risk-neutral investor cannot be a subject of the problem (3) in Section (2). He or she would choose to borrow without limit at the risk-free rate and invest the proceeds in the shares, leading to an unbounded objective in (3) (because the shares offer a positive risk premium, $E\left(R\right) > R_f$). Nonetheless m_{RN} is a member of each class $\mathbf{M}_n$ and particularly is a member of $\mathbf{M}_2$. The proof of Theorem 3 demonstrates for each n a series of risk-averse investors with a parametric marginal utility $m_{n,i} \subset \mathbf{M}_n$, $i = 1, 2, ...$, each with a bounded objective (3) such that $m_{n,i}$ converges pointwise to m_{RN}. For this reason the proof studies a series of values of the call option, one for each investor using $m_{n,i}$ as a stochastic discount factor. These values for the option converge to the bound C^u in (28), demonstrating that C^u is the supremum of option values within two-sided markets, and is the minimum option value in sellers-only markets. If call options were offered for sale at a price equal to or above C^u, all risk averse investors would be willing sellers and none would be a willing buyer.

The upper bound on a call option price C^u does not vary with the degree of dominance n and

the class of investors $\mathbf{M}_n$. This is unlike the case of the lower bound. Because the risk-neutral investor m_{RN} resides in each class, that investor represents the uniform upper bound. At the same time, the investors in the series $m_{n,i} \in \mathbf{M}_n$, $i = 1, 2, ...$ converging to m_{RN} are unusual; as index i increases, investor $m_{n,i}$ becomes increasingly concerned about risk in the increasingly far-left tail of the distribution of the share return R. These facts suggests the need for future analysis in which investors' Arrow-Pratt risk aversion coefficients are bounded from below. The potential benefit of these efforts is a tighter upper bound and a tighter range of option prices between the SD bounds.

An upper bound on a put option P^u is obtained using put-call parity, and in the same fashion as for the lower bound. It is

$$P^u = C^u - 1 + K/R_f.$$

This bound also is invariant to the degree of dominance n.

5.5 Option Bounds on a Share Basis

The lower and upper bounds introduced above are per dollar invested in the shares. To obtain a per-share basis instead, scale the prior values by the share price. The lower bounds are $C_n^l(S_0) = S_0 C_n^l$ and $P_n^l(S_0) = S_0 P_n^l$, and upper bounds are analogous.

6 Demonstrations of SD Bounds

We characterize and compare the SD bounds on option prices in this section, for degrees of dominance $n \geq 2$.[18] Our focus is the interaction between investors' risk attitudes and the location of risk in the distribution of returns, where differences in risk are captured by high-order moments of the return distribution F. Profiles of implied volatilities in our numerical analysis represent bounds on prices of options across exercise prices, where options are written on the SPX index; Figures 1(a) and 1(b) of the Introduction are examples. We document changes in IV profiles as the degree of dominance and moments of the return distribution change. For example, we compare the valuations of a call option (with a given exercise price) by risk-averse investors as a whole, on the one hand, to the valuations of the same option by prudent or temperate investors, on the other.

[18] Appendix D.2 presents additional numerical analyses, including the portfolios, v_1 and v_2 from the dual problem and comparative statics of the SD bounds with respect to the risk-free rate of interest.

Significant differences in valuation across investor classes are seen, and these differences vary with the degrees of downside risk and outside risk.

Because the range between upper and lower SD bounds widens as option tenor increases, we consider weekly options first and longer tenors later. This focus provides clarity in the analysis; it is easy to demonstrate the relationship between risk attitudes and risk location using IV profiles of short-dated options. In particular, it is easy to see the conditions under which a smile or smirk appears in an equilibrium IV profile, using the market interpretation of our model.

The SD bound on a call option with given exercise price requires three inputs: the distribution of gross returns F, the risk-free rate R_f, and the degree of dominance n. To calibrate F in our numerical analysis we estimate a conditional distribution of weekly S&P 500 (SPX) *log returns*, say, $F_{\ln}$ over the period 1990–2022. The exponential GARCH (EGARCH) model of Nelson (1993) is fit to weekly returns, where errors follow a skewed Student's t distribution (Hansen 1994), instead of a Generalized Error Distribution. This distribution $F_{\ln}$ is a function of four parameters representing jointly the mean, standard deviation, skewness and kurtosis of log returns. The resulting estimate $\widehat{F_{\ln}}$ may be asymmetric, as well as fat tailed. We also estimate the model under the Gaussian distribution as a point of comparison; it is a limiting case of the skewed t distribution in which skewness and excess kurtosis are zero. The baseline distribution F in our numerical analysis of SD bounds is obtained from the calibrated $F_{\ln}$ by change of variables.[19]

The SPX return data are from the Center for Research in Security Prices at the University of Chicago. Table 2 shows two sets of estimates of the first four moments of log returns, in one case assuming EGARCH errors are Gaussian, and in the other they follow the skewed t distribution. Importantly, the latter set of results shows that the SPX returns exhibit economically and statistically significant downside risk and excess tail (or outside) risk. The weekly risk-free rate in our calculations is the average duration-adjusted 3-month T-Bill yield from he Federal Reserve Board of Governors H.15 release. To be brief here, we report the details and the statistics of fit of the model, as well as further information on the data and our estimation in Appendix D.1.

Figures 1(a) and 1(b) plot SD bounds on weekly SPX call options ($T = 1/52$), assuming $F_{\ln}$ is Gaussian or a skewed t distribution, respectively. The option values in each figure are calculated

[19]The estimated standard deviation and the distribution $\widehat{F_{\ln}}$ of log returns are dynamic in the EGARCH model, representing weekly estimates. To calibrate $F_{\ln}$, which is not dynamic, we set the standard deviation of log returns equal to the sample average, and the other moments equal to the respective estimates.

Table 2
Estimated Moments from Log Returns Distribution

Notes: Moments of the returns distributions utilized in the numerical analysis. Weekly moments are from an EGARCH(1,1) model estimated on weekly returns data ranging from January 1990 to December 2022. Weekly skewness and kurtosis are computed using the estimated distributional parameters $(\hat{\lambda}, \hat{\eta})$ and the closed-form expressions for the standardized skewed Student's t distribution of Jondeau and Rockinger (2003), and their standard errors are obtained via the delta method. Moments from the one-month, three-month, six-month, and one-year returns distributions are obtained via Monte Carlo simulations using the estimated weekly returns distribution. Estimates of mean and volatility are annualized, and their standard deviations are in parentheses.

	Horizon (T)					
	1 week					
Moments	Gaussian	Skewed t	1 month	3 months	6 months	1 year
Mean	0.0676 (0.0215)	0.0640 (0.0207)	0.0597	0.0639	0.0637	0.0637
Volatility	0.154 (0.0691)	0.153 (0.0688)	0.151	0.163	0.166	0.167
Skewness	—	-0.507 (0.0847)	-0.981	-1.468	-1.590	-1.456
Kurtosis	—	4.013 (0.347)	6.197	8.969	9.541	8.204

using equation (17) of Theorem 2, and are reported as Black-Scholes implied volatilities. We see very different IV profiles in the two figures. The differences in the moments across the columns of Table 2 help to explain some of these results, while differences in investor risk attitudes explain others.

The second degree bound C_2^l is the minimum value of an option across the risk averse investors in $\mathbf{M}_2$. This class includes imprudent investors, who prefer downside to upside risk and who assess lower values to OTM options than do prudent investors.[20] In particular, imprudent investors may assign zero value to call options that are out-of-the-money. As a consequence, there is a large gap between C_2^l and C_3^l in each figure, and C_2^l is uniformly declining toward zero across options as the exercise price increases.[21]

An interesting and perhaps unexpected finding is that the third-degree lower bound C_3^l is a very good approximation of C_n^l, $n > 3$. The gap between C_3^l and C_{10}^l, for example, is tiny in each figure; it does not matter whether weekly returns follow a negatively skewed leptokurtotic distribution, as they do in our data, or follow the counterfactual Gaussian distribution. We see this result as well in other analyses not reported here; the gap between high degree bounds C_n^l and C_{n+1}^l, $n \geq 3$, is small for short-dated options, although the gaps widen as option tenor increases. These results

[20]The HARA class studied by Almeida and Freire (2022) includes examples of imprudent investors.

[21]The theory says that each lower SD bound $C_n^l = 0$ for $K/S_0 \geq g_n$, and each $n \geq 2$. Thus, C_3^l and C_{10}^l approach zero as K/S_0 increases. However the values g_3 and g_{10} are much larger than g_2, and are far above the range of K/S_0 in the figures (see Table 1).

suggest that in the pricing of SPX options, prudence is more influential than temperance or other high-order risk attitudes.

Figure 1(a) demonstrates the counterfactual case in which distribution $F_{\ln}$ is Gaussian and symmetric. Here the IV profiles representing third- and higher-degree SD lower bounds are level lines that appear to converge toward the BS IV as n increases. In other words, the third- and higher degree bounds are excellent approximations of the Black-Scholes price in the Gaussian environment, at least within the range of exercise prices shown in the figures.

When distribution $F_{\ln}$ is negatively skewed, as in our data, there is greater downside than upside risk in weekly SPX returns, and all risk-averse investors, including imprudent ones value options that hedge downside risk. For this reason, we see each of the lower bounds, C_2^l, C_3^l and C_{10}^l declines left to right in Figure 1(b), indicating higher implied volatilities for ITM than OTM calls (and by parity, higher IVs for OTM than ITM puts). At the same time, prudent investors are particularly averse to downside risks, and they put greater value on downside hedges. As a consequence, bounds C_3^l and C_{10}^l are above C_2^l.

While investors' risk attitudes are evidently an important driver of tighter or looser bounds for OTM call options, the bounds in Figure 1(a) do not resemble the IV profiles often observed in the SPX options. Similarly, the second-degree bound C_2^l in Figure 1(b) differs dramatically from C_3^l and C_{10}^l. In other words, neither the risk attitudes nor the nature of higher-degree risks alone is sufficient to explain observed IV profiles in index options. Instead, it is the interaction between these features of the option market that produces the familiar IV smirk and smile.

The figures suggest investors' aversion to outside risk does not meaningfully impact their valuation of options beyond their aversion to downside risk, at least insofar as short-dated options are concerned. There is little separation between C_3^l and C_4^l (and C_n^l, $n > 3$, more generally), and this is despite the fact our calibrated $F_{\ln}$ exhibits excess kurtosis (relative to the Gaussian distribution). Perhaps this is due to the asymmetry of an option's payoffs, in addition to its convexity. Long positions in call or put options may be used as bets on a rising (respectively, falling) share price. One conjecture is that bounds on straddles and strangles, which are portfolios of options, may show more sensitivity to the difference between prudence and temperance. These portfolios can be used as bets on high outside risk, paying off only when the share return is large in magnitude in either direction. At the same time, we note that bounds on the value of any portfolio is a simple weighted

sum the bounds on the options in the portfolio. If there is little difference between the bounds C_3^l and C_n^l, $n > 3$, why should the respective bounds on straddles and strangles differ? This is a topic for future work.

Our use of the skewed t distribution is advantageous. It leads to simple comparative-statics study of high-order risks. We vary skewness and the degree of downside risk while leaving kurtosis and other moments unchanged. Similarly, we vary kurtosis and the degree of outside risk while leaving skewness unchanged. Figures 3(a) and 3(b) demonstrate these effects by plotting the bounds C_3^l, and ignoring the other bounds, for now-obvious reasons; we have shown C_3^l provides an reasonable lower bound for all higher-degrees of dominance.

The IV profiles in the first figure represent three levels of skewness in the underlying distribution $F_{\ln}$. Downside risk varies across the profiles, while the kurtosis and the other moments do not; they are set at the baseline levels shown in Table 2. We see that the IV profile features a smirk when downside risk is high (relative to upside risk). If skewness is large and negative, the profile is mostly decreasing across exercise prices from left to right, and has a bowl in the region of OTM calls. Alternatively, the profile features a smile when the distribution is symmetric with zero skewness. Outside risk exists; $F_{\ln}$ is fat tailed with kurtosis above 3.0 in the baseline setting, and this explains why the zero-skewness profile is not a level line. In this case downside and upside risk are equal, but nonetheless the left edge of the bowl is slightly elevated relative to the right edge. The investors' prudence in this setting explains this slight asymmetry. Dislike of downside risk leads the investor to especially value ITM money calls and OTM puts, as these options might be used to reduce this risk.

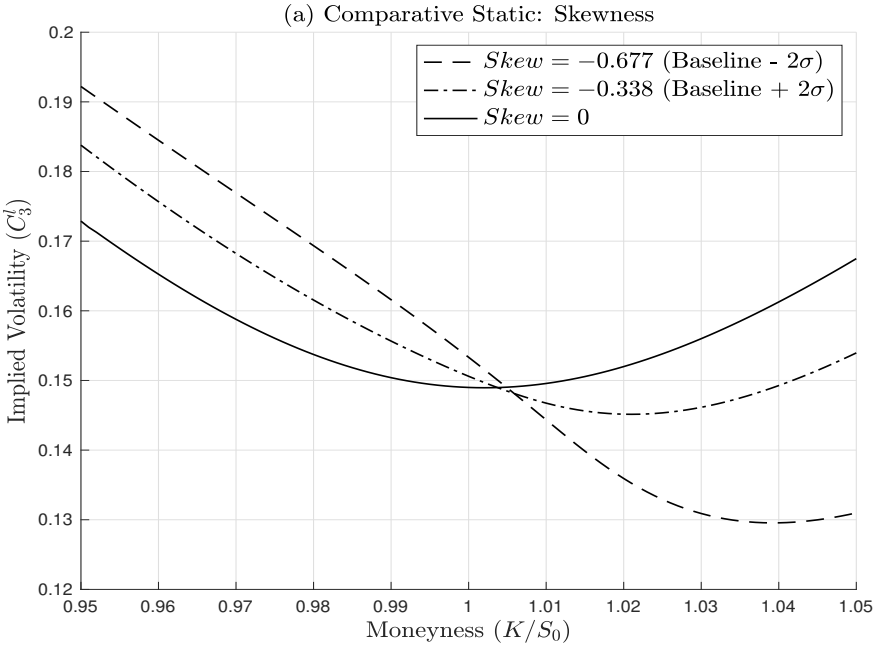
The second figure shows IV profiles in a similar fashion for two negatively skewed distributions that differ in the degree of outside risk. Now we see that the profile smirks when outside risk is high (kurtosis = 4.707), and that is a decreasing function of the exercise price when outside risk is low.

The alternative IV profiles in the figures are explained by differences in the location of risk in the distibution F, as well as the risk attitudes of investors. Generally speaking, the SD lower bounds of all degrees $n \geq 2$ rise and fall with the overall or total risk in the future returns of the underlying risky shares. In our numerical analysis, this risk is represented by the standard deviation of returns, which is held constant in the comparative static exercise. Therefore, total risk

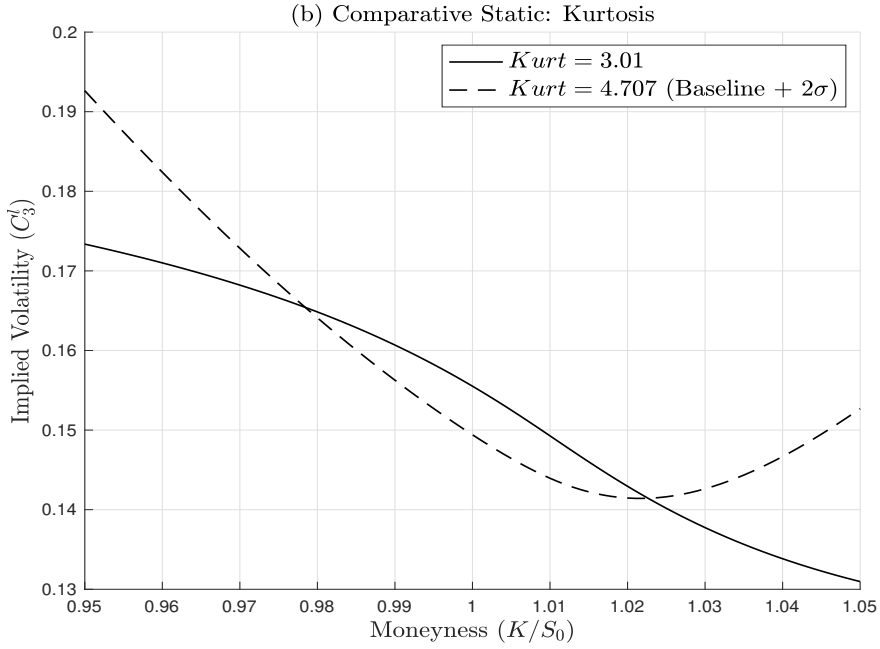
Figure 3
Stochastic Dominance Bounds on Weekly SPX Call Option
Higher-Order Risks in Weekly SPX Returns Distribution

Notes: This figure reports comparative statics on the skewness and kurtosis of the underlying SPX returns distribution and the corresponding effects on stochastic dominance bounds on call option implied volatilities. SPX log returns are assumed to follow a skewed Student's t distribution (Hansen 1994). The baseline conditional moments of this distribution are reported in the second column of Table 2 and the densities are overlaid for reference. The distributional parameters (η, λ) delivering the specified skewness and kurtosis are found via numerical methods using the expressions in Jondeau and Rockinger (2003). The lower and upper bounds are computed via (17) and (28). The risk-free rate is set at 2.5% per annum.

(a) Comparative Static: Skewness



(b) Comparative Static: Kurtosis



does not vary across the alternative profiles, but higher-order risk do vary. We estimate skewness and kurtosis as constants in our EGARCH model, and we are left to wonder if these might be estimated as dynamic factors that lead to dynamic SD bounds on options. This is a topic for future work.

Finally we provide estimates of the SD bounds on longer-dated options, with tenors $T = 4$, 13, 26 and 52 weeks. For this purpose, we use Monte Carlo simulation to produce multiple samples of T weekly returns (and weekly standard deviations) following the estimated weekly EGARCH model. Each return series is compounded, creating a sample of T-period returns, and the first four sample moments of the compounded returns are calculated. A skewed t distribution, say, $F_{\ln,T}$ is fit to these moments, one distribution for each T. This distribution is used to caluclate SD bounds for call options, for each of the four tenors, in the same manner as bounds for weekly returns. The details are in Appendix D.1, while Table 2 reports the four moments. Importantly, our estimates of skewness and kurtosis are within the range of other estimates in the literature (e.g., Neuberger and Payne 2021).

Figure 4 displays the upper and lower SD bounds on call option prices (for $n = 2, 3$ and 4), again as IV profiles, with one panel for each tenor. Because the standard deviation of returns grows with tenor, we plot IVs against the Black-Scholes option deltas Δ within the interval $[0.10, 0.90]$, instead of using exercise prices directly.

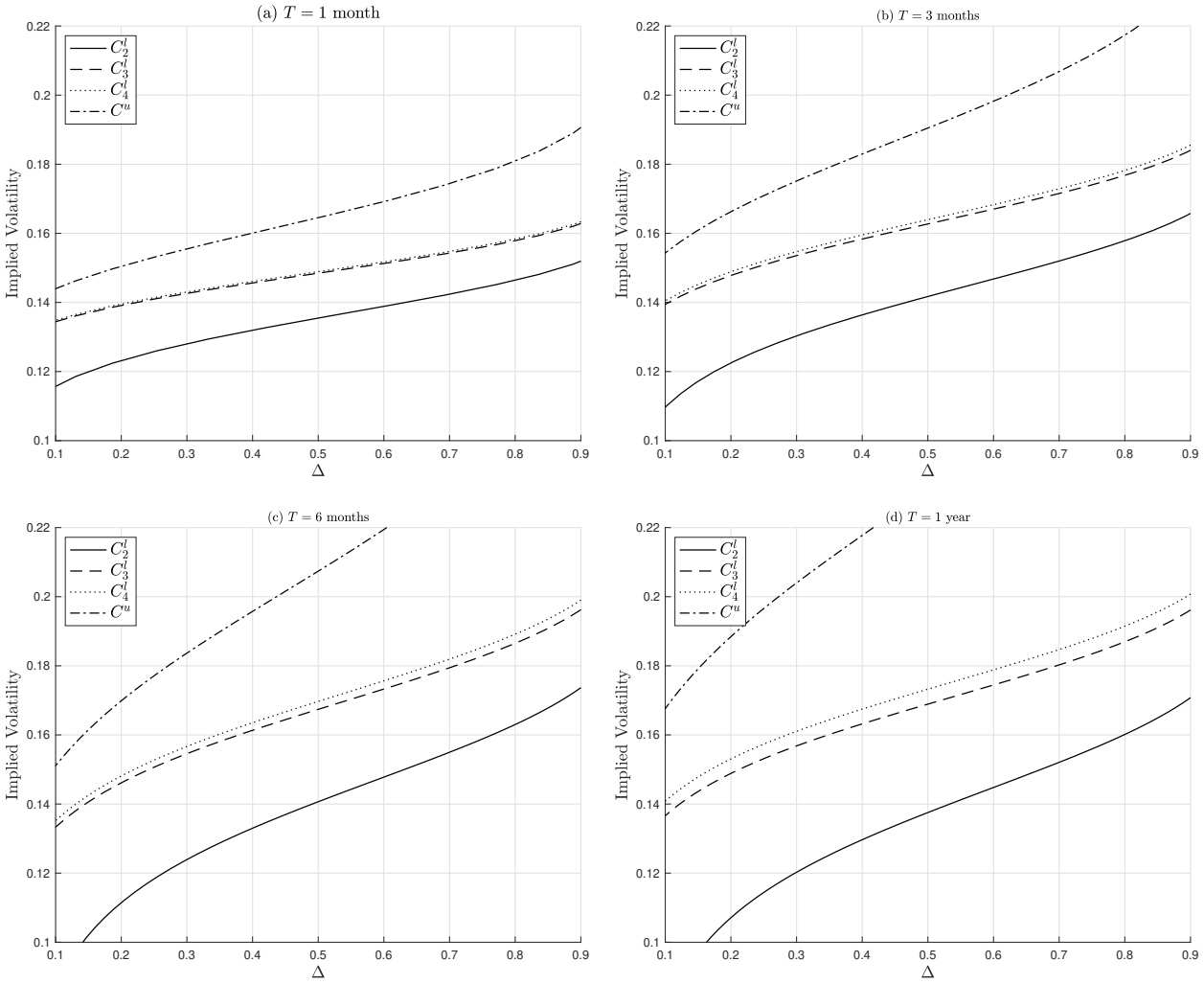
We see a very small gap between C_3^l and C_4^l for one and three-month options, and the gap increases modestly with tenor T across the panels. As with the weekly results, the figure suggests prudence is the dominant risk attitude (beyond the second-degree risk aversion) that governs option prices. Unlike the weekly results, however, we see no evidence of a smirk or smile in the figure. Instead, IVs increase with Δ, which is an inverse proxy for an option exercise price.[22]

These effects are best explained in the same manner as with weekly options, recognizing the relative magnitudes of downside and outside risks. According to Table 2 both the skewness and kurtosis of one-month returns are considerably larger than the respective moments for weekly returns, and the moments grow in magnitude up to six months and then level out. In other words, both downside risk and outside risk tend to rise with tenor, and the differences we observe between Figure 4 and the the previous figures (for weekly returns) are the consequence of a balance between

[22]The general character of the bounds in the figure are consistent the results of Almeda and Friere (2022).

Figure 4
Stochastic Dominance Bounds on Longer-Dated SPX Call Options

Notes: This figure reports the stochastic dominance bounds on longer-dated SPX call options. The distributions of SPX log returns over the horizon T are assumed to follow skewed Student's t distributions (Hansen 1994) whose moments are derived from simulations of weekly log returns, appropriately compounded (see Figure D.3). The conditional moments of the distributions are reported in Table 2 and the densities are overlaid for reference. For each T, the distributional parameters (η, λ) delivering the specified skewness and kurtosis are found via numerical methods using the expressions in Jondeau and Rockinger (2003) (see, also, Figure D.1). The lower and upper bounds are computed via (17) and (28). The risk-free rate is set at 2.5% per annum in each panel.



the risks. As of now, we have no specific formula to relate smile and smirks to the moments or risks in the distributions of returns, but sensitivity analyses lead to a couple of simple conclusions: Downside risk is of greater concern than outside risk in the distributions of monthly and longer returns. Prudent investors may choose to hedge this risk, bidding up prices (and IVs) of ITM calls and OTM puts in comparison to prices of other options of the same tenor. Thus, there is no smile/smirk in the respective IV profiles. However, the relative degree of outside risk compared to downside risk is greater in weekly returns, than in the other returns. In this case, prudent (and temperate) investors may choose to hedge this risk. This leads to a bowl in an IV profile; the IVs of OTM calls and ITM puts are above the near-the-money options.

7 Conclusion

This study introduced an economic theory offering new insights into the impact of investors' risk attitudes and beliefs on option prices. Our analysis revealed that investors' prudence, or aversion to downside risk, plays an important role in shaping equilibrium option prices. If investors additionally believe the underlying returns distribution is negatively skewed and leptokurtic, as our and other empirical analyses commonly indicate, then the resulting implied volatility profiles resemble the smiles and smirks regularly encountered in option data.

The implications of our findings extend beyond our theoretical contributions, as they open new directions for future research and practical applications. One area warranting further investigation is the extension of our model to dynamic market environments. Incorporating time-varying distributions of returns could enhance our understanding of how shifts in conditional skewness and kurtosis map to variation in option prices over time. From a methodological perspective, refining the upper bounds on option prices by constraining the Arrow-Pratt risk aversion coefficients of marginal investors could yield tighter price intervals and improve the model's alignment with observed market data. Additionally, our theory can be used to establish bounds on portfolios of options. Examples of interest include the VIX, which is a closely tracked index of the 30-day implied volatility on the S&P 500, and straddles or strangles, which involve bets on inside or outside risk. In the latter, the role of investors' fourth-degree risk attitudes, which differ from third-degree investors in the preference for inside rather than outside risk, might be more salient. Finally, our

analysis has practical implications for portfolio management and trading strategies. The use of SD bounds can serve as benchmarks for identifying mispriced options in the market from the perspective of investors with a particular risk profile, providing traders and investment managers with a tool for optimizing their portfolios.

Appendix A Preliminaries

Several preliminary results are stated here as lemmas, and are applied in work to follow. One goal is to demonstrate that values g_n, defined as the roots of (18), are increasing with the degree of dominance n. Lemma 1 describes the distribution functions $F_{n,g}$, $n \geq 2$ and $g \in (0, \infty)$, where

$$F_{n,g}(r) \overset{def}{=} \frac{1}{I_n(g)} \int_{x=0}^{r} (g-x)_+^{n-2} \, dF(x), \; r \in (0, \infty), \tag{A.1}$$

and the expectation operators $E_{n,g}$ under these distributions. (Setting $g = g_n$ in (A.1) gives the distribution F_n.) We show $F_{n,g}$ first-degree stochastically dominates $F_{n+1,g}$ in the sense of Quirk and Saposnik (1969). This means an investor with increasing utility (including one in $\mathbf{M}_2$) prefers a risky share following distribution $F_{n,g}$ over one following $F_{n+1,g}$. The second lemma shows that that the ratios $\frac{R_n(g)}{I_n(g)}$ and $\frac{C_n(g)}{I_n(g)}$ are increasing in g, and it demonstrates their limits as $g \to \infty$. A third lemma shows $g_{n+1} > g_n$, $n \geq 2$.

Lemma 1. For each $n \geq 2$ and $g \in (0, \infty)$, $F_{n,g}$ first-degree stochastically dominates (FSD) $F_{n+1,g}$, and does so strictly. This means

$$F_{n+1,g}(r) - F_{n,g}(r) > 0, \; r \in (0, g), \tag{A.2}$$

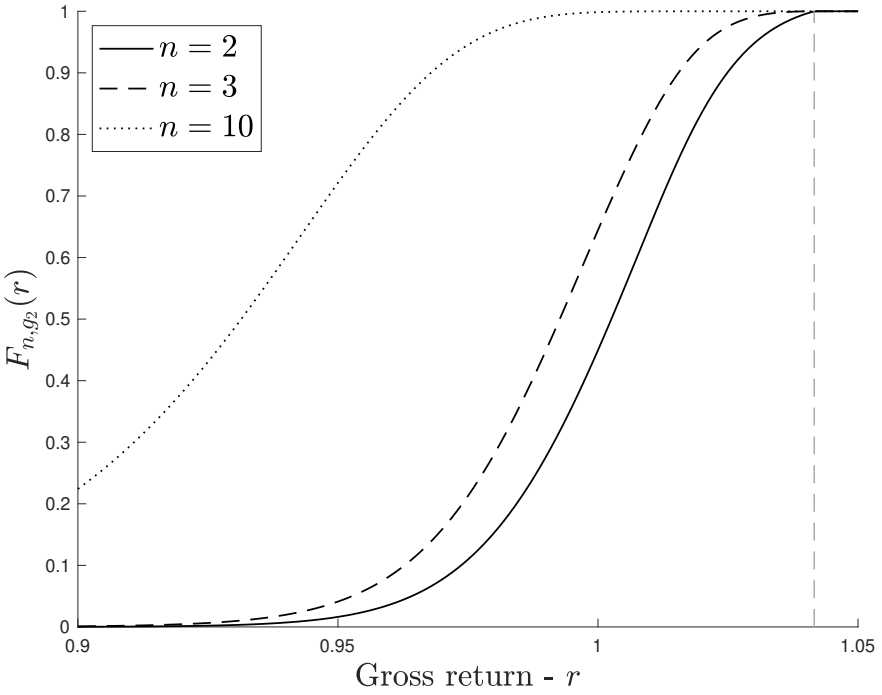
Figure A.1 demonstrates examples of FSD, plotting distributions $F_{n,g}$ for degrees of dominance $n = 2$, 3 and 10, and setting $g = g_2 = 1.042$. It is evident that $F_{10,g}(r) > F_{3,g}(r) > F_{2,g}(r)$ for all $r(0, \infty)$. Every investor holding the risky share (in isolation) prefers $F_{2,g}$ over the other distributions because it assigns higher likelihoods to large return outcomes.

Proof: The definition (A.1) implies $F_{n+1,g}(r) - F_{n,g}(r) = 0$ if either $r = 0$ or $r \geq g$. Using the definition $I_n(g) = E_F\left((g-R)_+^{n-2}\right)$ we obtain

$$\begin{aligned} F_{n+1,g}(r) - F_{n,g}(r) &= \frac{1}{I_{n+1}(g)} \int_{x=0}^{r} (g-x)_+^{n-1} \, dF(x) - \frac{1}{I_n(g)} \int_{x=0}^{r} (g-x)_+^{n-2} \, dF(x) \\ &= \int_{x=0}^{r} \left(\frac{I_n(g)}{I_{n+1}(g)} (g-x) - 1 \right) dF_{n,g}(x) \\ &= \int_{x=0}^{r} \left(\frac{g-x}{g - E_{n,g}(R)} - 1 \right) dF_{n,g}(x). \end{aligned} \tag{A.3}$$

Figure A.1
Distributions F_{n,g_2} for $n = 2, 3, 4$

Notes: This figure plots the distributions $F_{n,g}$ for $n = 2, 3$ and 4 for a select value of $g = g_2 = 1.042$. The distribution F is skewed t with moments given in the second column of Table 2. A vertical dashed line is drawn at $r = g_2$.



Because $0 < E_{n,g}(R) < g$, and because distribution $F_{n,g}$ is strictly increasing on $(0, g)$, an increment of this difference is

$$d\left(F_{n+1,g}(r) - F_{n,g}(r)\right) \begin{cases} > 0 & \text{if } 0 < r < E_{n,g}(R), \\ = 0 & \text{if } r = E_{n,g}(R) \text{ or } r \geq g, \\ < 0 & \text{if } E_{n,g}(R) < r < g. \end{cases}$$

The inequality (A.2) holds strictly as a consequence. QED

Several useful results follow from strict FSD for the case $g > K$. These are in

Lemma 2 - For each $n \geq 2$ and $g > K$,

$$E_{n,g}(c(R)) > E_{n+1,g}(c(R)),\ E_{n,g}(p(R)) < E_{n+1,g}(p(R)),\ E_{n,g}(R) > E_{n+1,g}(R), \tag{A.4}$$

$$\frac{d}{dg}E_{n,g}(c(R)) > 0,\ \frac{d}{dg}E_{n,g}(p(R)) < 0,\ \frac{d}{dg}E_{n,g}(R) > 0, \tag{A.5}$$

$$E_{n,g}\left(c\left(R\right)\right) \underset{g\to\infty}{\to} E_F\left(c\left(R\right)\right),\ E_{n,g}\left(p\left(R\right)\right) \underset{g\to\infty}{\to} E_F\left(p\left(R\right)\right),\ E_{n,g}\left(R\right) \underset{g\to\infty}{\to} E_F\left(R\right). \tag{A.6}$$

Importantly, the inequalities of Lemma 2 are *not* equivalent to comparisons under the distributions F_n and F_{n+1}, because $g_n \neq g_{n+1}$. The expectations are defined by ratios,

$$E_{n,g}\left(c\left(R\right)\right) = \frac{C_n\left(g\right)}{I_n\left(g\right)},\ E_{n,g}\left(p\left(R\right)\right) = \frac{P_n\left(g\right)}{I_n\left(g\right)} \text{ and } E_{n,g}\left(R\right) = \frac{R_n\left(g\right)}{I_n\left(g\right)}, \tag{A.7}$$

so the comparisons of Lemma 2 apply equivalently to the respective ratios.

Proof: We demonstrate the results in (A.4)-(A.6) for the share return R, $n > 2$; those for $c\left(R\right)$ and $p\left(R\right)$, and for the cases $n = 2$ follow similarly. Because the inequality of distributions (A.2) holds, so does the inequality of expectations $E_{n,g}\left(R\right) > E_{n+1,g}\left(R\right)$. Using the final equality in (A.7),

$$E_{n,g}\left(R\right) = \int_{x=0}^{g} x dF_{n,g}\left(x\right) = \frac{\int_{x=0}^{g} x\left(1-\frac{x}{g}\right)^{n-2} dF\left(x\right)}{\int_{x=0}^{g}\left(1-\frac{x}{g}\right)^{n-2} dF\left(x\right)} \underset{g\to\infty}{\to} E_F\left(R\right),$$

and

$$\begin{aligned}
\frac{d}{dg}E_{n,g}\left(R\right) &= \left(n-2\right)\frac{I_{n-1}\left(g\right)}{I_n\left(g\right)}\left(\frac{\int_{x=0}^{g} x\left(g-x\right)^{n-3} dF\left(x\right)}{\int_{x=0}^{g}\left(g-x\right)^{n-3} dF\left(x\right)} - \frac{\int_{x=0}^{g} x\left(g-x\right)^{n-2} dF\left(x\right)}{\left(\int_{x=0}^{g}\left(g-x\right)^{n-2} dF\left(x\right)\right)^2}\right) \\
&= \left(n-2\right)\frac{E_{n-1,g}\left(R\right) - E_{n,g}\left(R\right)}{g - E_{n-1,g}\left(R\right)} \\
&> 0,
\end{aligned}$$

where the inequality follows from (A.2) and $g > E_{n-1,g}\left(R\right)$. QED

We use Lemma 2 to prove

Lemma 3 - For each $n \geq 2$, $g_{n+1} > g_n > R_f$.

Proof: The value g_n is defined as the root of

$$E_{n,g}\left(R\right) = \int_{x=0}^{g} x dF_{n,g}\left(x\right) = R_f$$

in Theorem 2. The second equality implies $g_n > R_f$. The inequalities (A.4) and the monotonicity demonstrated in Lemma 2 together imply $g_{n+1} > g_n$. QED

Appendix B Theorems 1, 2 and 4

The proofs of the Theorems 1,2 and 4 are in this appendix, together with statements of the revised primal and dual optimization problems discussed in Section 3. The revisions rely on a substitution for the discount factor m using the equation (6) of Theorem 1. A proof of Theorem 3 appears in the following appendix.

B.1 Proof of Theorem 1

We rely on Williamson's characterization of p-times monotone functions to derive our equation (14). This is in:

Williamson (see his Theorem 1). A necessary and sufficient condition that $m(r)$, $r > 0$, *be* $(n-1)$*-times monotone is*

$$m(r) = \int_{v=0}^{\infty} (1 - vr)_{+}^{n-2} \, d\varphi(v), \; r \in (0, \infty), \tag{B.1}$$

where the function $\varphi(v)$ *is increasing, bounded below and may be discontinuous at* $v = 0$, *and where* $(x)_{+} \overset{def}{=} x$ *or* 0 *if* $x > 0$ *or* ≤ 0, *respectively.*

Proof of Theorem 1: Because φ is bounded below, let $\varphi(0) = 0$ without loss of generality. After substitution of variables $v = 1/g$, $g \in (0, \infty)$ we obtain

$$\begin{aligned} m(r) &= \overline{m} + \int_{g=\infty}^{0} m_{n,g}(r) \, g^{2-n} d\varphi(1/g), r \in (0, \infty) \\ &= \overline{m} + \int_{g=0}^{\infty} m_{n,g}(r) \, dy(g), \; r \in (0, \infty), \end{aligned} \tag{B.2}$$

where

$$y(g) = -\int_{x=0}^{g} x^{2-n} d\varphi(1/x) \tag{B.3}$$

and $\overline{m} > 0$ or $= 0$ depending on whether $\lim_{g \to \infty} \varphi(1/g) > 0$ or $= 0$, repectively. Function y is increasing in $g \in (0, \infty)$, and we have equality (14). QED.

Comments: For each $n \geq 2$, the class of marginal utilities $\mathbf{M}_n$ is a convex cone For any two members m_1,m_2 of $\mathbf{M}_n$ that satisfy (14), the convex combination also is a member; if $a, b \geq 0$

then $am_1 + bm_2 \in \mathbf{M}_n$. The elements of $\mathbf{G}_n$ are members of $\mathbf{M}_n$, and are sufficient to generate $\mathbf{M}_n$. Equality (B.2) represents a convex combination of members of $\mathbf{G}_n$ (using integration), and it represents all $m \in \mathbf{M}_n$.

The integral in (B.2) declines to zero as r increases,

$$\int_{g=0}^{\infty} (g-r)_+^{n-2} \, dy\,(g) \underset{r\to\infty}{=} 0,$$

and limiting marginal utility is $\overline{m} \overset{def}{=} \lim_{r\to\infty} m_n(r)$. If an investor's utility function is power or exponential then $\overline{m} = 0$, while for a risk neutral investor $\overline{m} > 0$.

Williamson's characterization allows $\varphi = \varphi_1 + \varphi_2$ where φ_1 and φ_2 are absolutely continuous and discrete functions respectively; φ may have a countable number of positive mass points. As a consequence, the function y in (B.3) may have mass points. An example is the the function defined in (19) as the solution to the lower bound in Theorem 2.

B.2 Revised Primal and Dual Problems

The choice variables in the optimization problems of Section 3 are discount factors $m \in \mathbf{M}_n$. To solve (8) and (9) we substitute for m using the equality (14), and then reverse the order of integrations. The revised primal for the lower bound of a call option is

$$\min_{\overline{m}\geq 0, y\in\mathbf{M}_1} \overline{m} E_F(c(R)) + \int_{g=0}^{\infty} C_n(g)\, dy(g) \tag{B.4}$$

subject to

$$1 = \overline{m} R_f + R_f \int_{g=0}^{\infty} I_n(g)\, dy(g), \tag{B.5}$$

$$1 = \overline{m} E_F(R) + \int_{g=0}^{\infty} R_n(g)\, dy(g). \tag{B.6}$$

Problem (B.4) minimizes the value of a call option, as does problem (8), but now a weighted sum of discounted values of future payoffs defines the objective, one value for each investor in $\mathbf{G}_n$. The positive $\overline{m}$ and increments of y are the weights in this sum. In the constraints (B.5) and (B.6), weighted sums of the present values of the bond and shares (using members of $\mathbf{G}_n$ as discount factors) are set to one. The revised primal for the upper bound appears similarly, but with an

objective to find a supremum instead of a minimum.

We treat the dual problem for the lower bound on the call option as we do the primal by substituting for m using (14) and exchanging integrals. It is now

$$\max_{v_1,v_2} v_1 + v_2 \tag{B.7}$$

subject to

$$\frac{C_n(g)}{I_n(g)} \geq v_1 \frac{R_n(g)}{I_n(g)} + v_2 R_f,\ g \in (0,\infty). \tag{B.8}$$

and

$$E_F(c(R)) \geq v_1 E_F(R) + v_2 R_f. \tag{B.9}$$

The objective is the same as in (9) while the constraints are simplified; they are now a collection of inequalities representing dominance within a class of simple parametric functions in $\mathbf{G}_n$ instead of within $\mathbf{M}_n$. When (B.8) and (B.9) hold, each investor in $\mathbf{G}_n$ prefers to purchase the call option (at the margin) over buying the portfolio v_1, v_2 of only the bond and shares. The dual for the upper bound is explained similarly. It minimizes the portfolio value subject to reversed inequalities that say each investor in $\mathbf{G}_n$ prefers the portfolio to the call option.

The constraint (B.9) of the dual (for the lower bound) is redundant, and similarly the reversed constraint for the upper bound is redundant. To see this result for either bound, consider the limits stated in Lemma 2 and the equalities of expectations and ratios in (A.7). These results demonstrate that each ratio in (B.8) converges to the respective expected value in (B.9) as g increases without limit. Thus (B.9) is implied by the inequalities (for all $g > 0$) in (B.8) for the lower bound, and the analogous result holds for the upper bound. As a consequence, we ignore the constraint (B.9) in the dual problem for the lower bound, and we proceed similarly for the upper bound.

B.3 Convexity Introduced

To prove Theorems 2 and 4 we require the ratio $\frac{C_n(g)}{I_n(g)R_f}$ to be convex as an implicit function of $\frac{R_n(g)}{I_n(g)R_f}$. Convexity is proved for $n = 2$ in the following section, while for $n > 2$ we provide numerical demonstration of convexity.[23] The use of the convex relation is evident in the proofs.

[23]Ritchken (1985) also proves convexity for $n = 2$, but he does so under different conditions. His state space is discrete while ours is continuous, and he interprets his method as a substitution of variables in a linear program,

It allows us to conclude that a single investor $m_{n,g} \in \mathbf{G}_n$ acts a representative agent, and to find lower bounds of the call and put prices as values of future payoffs using $m_{n,g}$ as a discount factor. This is true for all option exercise prices K.

Convexity is explained as follows. The constraints (B.8) of the dual problem are rewritten

$$H_n\left(J_n\left(\theta\right)\right) \geq v_1\theta + v_2,\ \theta \in \left(0, \frac{E_F\left(R\right)}{R_f}\right), \tag{B.10}$$

where H_n is the continuous function

$$H_n\left(g\right) = \frac{C_n\left(g\right)}{I_n\left(g\right)R_f},\ g \in \left(0,\infty\right),$$

and J_n is the continuous implicit inverse function,

$$J_n\left(\theta\right) = \left\{g : \frac{R_n\left(g\right)}{I_n\left(g\right)R_f} = \theta\right\},\ \theta \in \left(0, \frac{E_F\left(R\right)}{R_f}\right). \tag{B.11}$$

The function J_n exists and the substitution of variables is proper because the ratio $\frac{R_n(g)}{I_n(g)}$ is continuous, strictly increasing and bounded on $(0,\infty)$ with limiting values

$$\lim_{g\to\infty} \frac{R_n\left(g\right)}{I_n\left(g\right)} = E_F\left(R\right),\ \text{and}\ \lim_{g\to 0} \frac{R_n\left(g\right)}{I_n\left(g\right)} = 0,\ \text{for all}\ n \geq 2. \tag{B.12}$$

See Lemma 2. Similarly H_n is increasing with limiting values

$$\lim_{g\to\infty} \frac{C_n\left(g\right)}{I_n\left(g\right)} = E_F\left(c\left(R\right)\right),\ \text{and}\ \lim_{g\to 0} \frac{C_n\left(g\right)}{I_n\left(g\right)} = 0,\quad \text{for all}\ n \geq 2. \tag{B.13}$$

In the proofs of Theorems 2 and 4 we assume

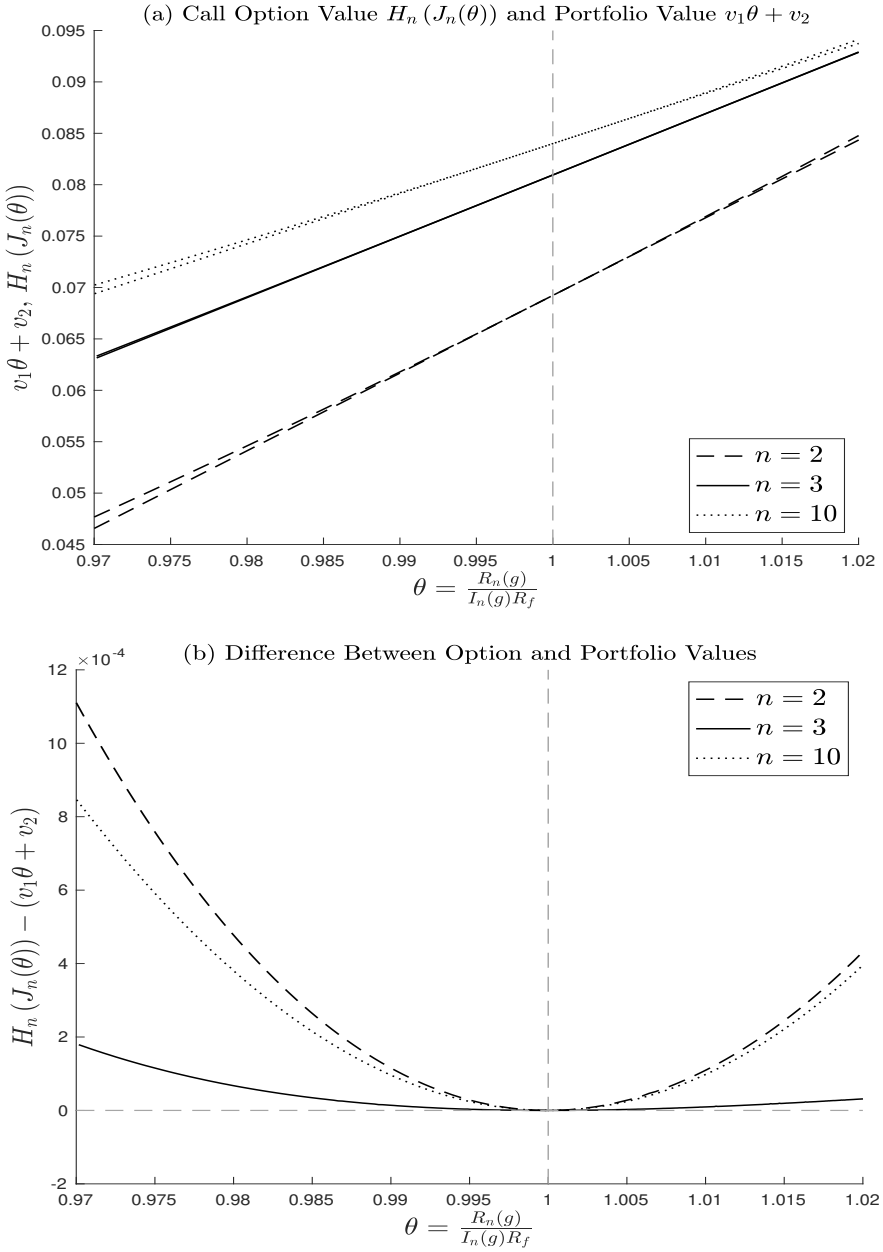
Convexity. The compound function $H_n \circ J_n$ defined in (B.10) and (B.11) is convex.

Figure B.1 demonstrates the role of convexity in the dual problem and its solution. The first figure plots the right- and left-hand sides of the inequality (B.10) as solid and dashed lines, respectively, representing the values of the call option $H_n\left(J_n\left(\theta\right)\right)$ and the portfolio $v_1\theta + v_2$, while the second plots the difference between the two sides. These values are plotted against θ. These

while we interpret the result using generating classes of marginal utilities.

Figure B.1
Numerical Demonstration of Convexity

Notes: This figure demonstrates convexity on a one-year call option. The distribution F is skewed t with moments reported in the last column of Table 2. In Figure B.1(a), the portfolio value $v_1\theta + v_2$ appears as a straight line with intercept v_2 and slope v_1, below the bowl-shaped call option value $H_n\left(J_n(\theta)\right)$. Figure B.1(b) plots the difference between the option and portfolio values. Vertical lines are drawn in each figure at the point of tangency, $\theta = 1$.



items $H_n(J_n(\theta))$, $v_1\theta + v_2$ and θ are the time 0 discounted value of future payoffs for the option, portfolio and share, respectively, one value each for each investor $m_{n,g} \in \mathbf{G}_n$. (Because $\theta = \frac{R_n(g)}{I_n(g)R_f}$ is a continuous and increasing function, each point in a figure is associated with one and only one index value g.) In other words, figures present three cross sectional profiles of invesotors' valuations, one profile for each of the degrees of dominance $n = 2$, 3 and 10.

For each degree of dominance, there is a single point of tangency of $H_n(J_n(\theta))$ and $v_1\theta + v_2$. This point of tangency occurs at $\theta = \frac{R_n(g)}{I_n(g)R_f} = 1$, which is the equality (18).

Given a strictly convex function $H_n \circ J_n$, there is a single $g \in (0, \infty)$ at which the constraint (B.10) holds as an equality, and otherwise is a strict inequality. Figure B.1 demonstrates this idea, using degrees of dominance $n = 2$, 3 and 10. Figure B.1(a) plots the left and right-hand sides of (B.10) individually, with $H_n(J_n(\theta))$ and while Figure B.1(b) plots the difference. In each figure there is a single point of tangency at $\theta = 1$, and otherwise the difference is positive.

B.4 Convexity Proved ($n = 2$) and Demonstrated ($n > 2$)

The proofs of Theorems 2 and 4 assume the compound function $H_n \circ J_n$ is convex. Here we prove convexity for $n = 2$. We develop analytic expressions for the first and second derivatives of $H_n \circ J_n$, which are simple functions of the moments C_n, P_n, R_n, and I_n, and show a positive second derivative. For $n > 2$, we derive the conditions under which the second derivative is positive.

The prior section introduces H_n and J_n as continuous functions on their domains $(0, \infty)$ and $(0, E_F(R)/R_f)$, respectively, so $H_n \circ J_n$ also is continuous. Furthermore, $H_n \circ J_n = 0$ on the interval $(0, K)$ (because $C_n = 0$). For this reason the following analysis focuses on $g > K$, demonstrating a positive second derivative on (K, ∞).

For each $g > K$

$$\begin{aligned} \frac{d}{d\theta} H_n(J_n(\theta))\Big|_{\theta=\frac{R_n(g)}{I_n(g)R_f}} &= \frac{d}{dg} H_n(g) \times \frac{d}{d\theta} J_n(\theta)\Big|_{\theta=\frac{R_n(g)}{I_n(g)R_f}} \\ &= \frac{d}{dg}\frac{C_n(g)}{I_n(g)} \Big/ \frac{d}{dg}\frac{R_n(g)}{I_n(g)} \\ &= 1 + h_n(g) \end{aligned} \tag{B.14}$$

where

$$h_n(g) \stackrel{def}{=} \frac{d}{dg}\frac{P_n(g)}{I_n(g)} \Big/ \frac{d}{dg}\frac{R_n(g)}{I_n(g)} \tag{B.15}$$

The first equality follows from the chain rule of calculus and the definition (B.11), and the second equality from the derivative of an inverse function. The third equality uses put-call parity of payoffs, which leads to

$$1 + \frac{\frac{d}{dg}\frac{P_n(g)}{I_n(g)}}{\frac{d}{dg}\frac{R_n(g)}{I_n(g)}} = \frac{\frac{d}{dg}\frac{C_n(g)}{I_n(g)}}{\frac{d}{dg}\frac{R_n(g)}{I_n(g)}} > 0.$$

The inequality follows from Lemma 2, and it demonstrates a positive first derivative.

Using similar logic

$$\frac{d^2}{d\theta^2} H_n\left(J_n(\theta)\right)\Big|_{\theta=\frac{R_n(g)}{I_n(g)R_f}} = \frac{d}{dg}h_n(g) \Big/ \frac{d}{dg}\frac{R_n(g)}{I_n(g)}. \tag{B.16}$$

We need only evaluate the numerator $\frac{d}{dg}h_n(g)$ in (B.16) to demonstrate convexity. The denominator is shown positive in Lemma 2. For $n = 2$ we prove $\frac{d}{dg}h_n(g) > 0$, while for $n > 2$ we derive analytic expressions for this derivative and Figure B.1 above demonstrates numerically that it is positive, using the baseline values of the analysis in Section 6.

We consider the cases $n = 2$ and > 2 separately. For $n = 2$

$$\frac{d}{dg}\frac{P_2(g)}{I_2(g)} = -\frac{dF(g)}{F(g)^2}\int_{r=0}^{K}(K-r)\,dF(r), \text{ and} \tag{B.17}$$

$$\frac{d}{dg}\frac{R_2(g)}{I_2(g)} = \frac{dF(g)}{F(g)^2}\int_{r=0}^{g}(g-r)\,dF(r). \tag{B.18}$$

These results lead to

Proposition 1 - Convexity $n = 2$. The function $H_2 \circ J_2$ is convex.

Proof. The derivative of h_2 is

$$\begin{aligned}\frac{d}{dg}h_2(g) &= \frac{d}{dg}\left(-\int_{r=0}^{K}(K-r)\,dF(r)\Big/\int_{r=0}^{g}(g-r)\,dF(r)\right)\\ &= \frac{\int_{r=0}^{K}(K-r)\,dF(r)}{\left(\int_{r=0}^{g}(g-r)\,dF(r)\right)^2}F(g)\\ &> 0\end{aligned}$$

Because $\frac{R_2(g)}{I_2(g)}$ is increasing in g (Lemma 2), the denominator in (B.16) is positive. We conclude $\frac{d^2}{d\theta^2}H_2(J_2(\theta))_{\theta=\frac{R_2(g)}{I_2(g)R_f}} > 0$ for $g > K$, and having shown $H_2 \circ J_2 = 0$ for $g \leq 0$ we conclude $H_2 \circ J_2$ is convex. QED

If $n > 2$,

$$\frac{d}{dg}\frac{P_n(g)}{I_n(g)} = (n-2)\frac{I_{n-1}(g)}{I_n(g)}\left(\frac{P_{n-1}(g)}{I_{n-1}(g)} - \frac{P_n(g)}{I_n(g)}\right), \tag{B.19}$$

$$\frac{d}{dg}\frac{R_n(g)}{I_n(g)} = (n-2)\frac{I_{n-1}(g)}{I_n(g)}\left(\frac{R_{n-1}(g)}{I_{n-1}(g)} - \frac{R_n(g)}{I_n(g)}\right), \tag{B.20}$$

leading to

$$h_n(g) = \left(\frac{P_{n-1}(g)}{I_{n-1}(g)} - \frac{P_n(g)}{I_n(g)}\right)\Big/\left(\frac{R_{n-1}(g)}{I_{n-1}(g)} - \frac{R_n(g)}{I_n(g)}\right). \tag{B.21}$$

Again, $H_n \circ J_n$ is convex if and only if $sign\left(\frac{d}{dg}h_n(g)\right) \geq 0$. To facilitate numerical work, we derive $\frac{dh_n(g)}{dg}$ as a simple function of the moments P_n, I_n and R_n .

Proposition 2 − Convexity $n \geq 3$. The function $H_n \circ J_n$ is convex on $(0,\infty)$, with a positive second derivative on $g > K$, if and only if $h_{n-1}(g) - h_n(g) > 0$ for all $g \in (K,\infty)$, where $h_n(g)$ is given in equation (B.21).

Proof. We have shown $H_n \circ J_n$ is continuous on $(0,\infty)$, and is zero on $(0,K)$. To establish $H_n \circ J_n$ *is convex on* $(0,\infty)$ it is sufficient to show $h_n(g)$ is strictly increasing on (K,∞). The first

derivative for $n \geq 3$ is

$$\begin{aligned}\frac{d}{dg}h_n(g) &= \frac{d}{dg}\left(\frac{\frac{P_{n-1}(g)}{I_{n-1}(g)} - \frac{P_n(g)}{I_n(g)}}{\frac{R_{n-1}(g)}{I_{n-1}(g)} - \frac{R_n(g)}{I_n(g)}}\right) \\ &= \frac{\left(\frac{R_{n-1}(g)}{I_{n-1}(g)} - \frac{R_n(g)}{I_n(g)}\right)\frac{d}{dg}\left(\frac{P_{n-1}(g)}{I_{n-1}(g)} - \frac{P_n(g)}{I_n(g)}\right) - \left(\frac{P_{n-1}(g)}{I_{n-1}(g)} - \frac{P_n(g)}{I_n(g)}\right)\frac{d}{dg}\left(\frac{R_{n-1}(g)}{I_{n-1}(g)} - \frac{R_n(g)}{I_n(g)}\right)}{\left(\frac{R_{n-1}(g)}{I_{n-1}(g)} - \frac{R_n(g)}{I_n(g)}\right)^2}\end{aligned}$$

Using the equalities (B.17)-(B.21), this resolves to

$$\frac{d}{dg}h_n(g) = \Gamma_n(g) \times (h_{n-1}(g) - h_n(g))$$

where

$$\Gamma_n(g) = \begin{cases} \frac{dF(g)}{F(g)}\frac{g - \frac{R_2(g)}{I_2(g)}}{\frac{R_2(g)}{I_2(g)} - \frac{R_3(g)}{I_3(g)}} & \text{if } n = 3 \\ (n-3)\frac{I_{n-2}(g)}{I_{n-1}(g)}\frac{\frac{R_{n-2}(g)}{I_{n-2}(g)} - \frac{R_{n-1}(g)}{I_{n-1}(g)}}{\frac{R_{n-1}(g)}{I_{n-1}(g)} - \frac{R_n(g)}{I_n(g)}} & \text{if } n > 3. \end{cases}$$

The inequality $\Gamma_n(g) > 0$ (for all $n \geq 3$ and $g \in (K, \infty)$) follows from Lemma 2 and a strictly increasing physical distribution, $dF > 0$. Thus, the sign of the second derivative of $H_n \circ J_n$ is determined by the difference $h_{n-1}(g) - h_n(g)$. QED

B.5 Proof of Theorem 2

The first step in the proof demonstrates that a substitution of the marginal utility (19) into the objective (B.4) produces the lower bound C_n^l that appears in equation (17). This step also shows (19) satisfies the constraints (B.5) and (B.6). A second step demonstrates that the portfolio in (20) and (21) satisfies the dominance constraints (B.10), and that the value of this portfolio is (17), confirming strong duality of the solutions. The convexity of function $H_n \circ J_n$ plays an important role in demonstrating the inequalities (B.10).

Proof. Consider first the primal (B.4). To verify C_n^l in equation (17) is the solution, substitute for $\overline{m}$ and y in the objective (B.4) using equations (19), and then integrate. To verify the primal constraints are satisfied, substitute and integrate in (B.5) and (B.6).

Now focus on the dual. The candidate portfolio in (20) and (21) gives $v_1 + v_2 = C_n^l$. To demonstrate strong duality, we must show the candidate portfolio satisfies the constraints (B.10). Consider two cases $g_n \leq K$ and $g_n > K$. If $g_n \leq K$: (a) $C_n(g_n) = C_n^l = 0$ using (16), and (b) $v_1 = v_2 = 0$, using (20) and (21). Thus (B.10) holds. If $g_n > K$ instead, consider both the level and the first the derivative with respect to θ of the difference between the left and right sides of the constraint (B.10), evaluated at $\theta = \theta_n \overset{def}{=} \frac{R_n(g_n)}{I_n(g_n)R_f}$. The level is

$$\begin{aligned} H_n(J_n(\theta_n)) - v_1\theta_n - v_2 &= \frac{C_n(g_n)}{I_n(g_n)R_f} - v_1\frac{R_n(g_n)}{I_n(g_n)R_f} - v_2 \\ &= C_n^l - v_1 - v_2 \\ &= 0 \end{aligned} \tag{B.22}$$

The first equality follows from the definition of the functions H_n and J_n, the second equality follows from (17) together with g_n as the root of (18), and final equality follows from the definition of the candidate portfolio in (20) and (21). We conclude that the constraint (B.10) holds as an equality at θ_n.

Following the logic of Section B.3 and using (20), the derivative of the difference is

$$\begin{aligned} \frac{d}{d\theta}H_n(J_n(\theta))\Big|_{\theta=\theta_n} - v_1 &= \frac{d}{dg}\frac{C_n(g)}{I_n(g)} \Big/ \frac{d}{dg}\frac{R_n(g)}{I_n(g)}\Big|_{g=g_n} - v_1 \\ &= 0. \end{aligned} \tag{B.23}$$

Because $H_n \circ J_n$ is convex, the equalities (B.22) and (B.23) imply $H_n\left(J_n\left(\theta\right)\right) - v_1\theta - v_2$ reaches a global minimum of zero on $(0, E\left(R\right))$ at θ_n. Therefore the dual constraint (B.10) is satisfied for all $\theta \in (0, E\left(R\right))$ when it is evaluated using the candidate portfolio v_1, v_2. Strong duality holds: The candidate solutions to the primal and the dual are equivalent and are optimal solutions. QED

B.6 Proof of Theorem 4

Risk-neutral investors with constant marginal utility are members of $\mathbf{M}_2$, and Theorem 4 says upper bounds on call option prices are defined by a particular risk-neutral discount factor $m_{RN} = 1/E_F\left(R\right)$. But a risk-neutral investor cannot be the subject of the problem (3); the objective is unbounded for this investor. For these reasons, the following proof introduces for each $n \geq 2$ a series of risk-averse investors with discount factors $m_n^i \in \mathbf{M}_n$ converging to m_{RN}. Each of these investors satisfies the constraints of (3) and has a bounded objective. The proof demonstrates that an upper bound is the supremum of a series of call option values using m_n^i, $i \to \infty$, as discount factors.

Proof. Consider first the dual problem, and portfolio (29) as a candidate solution to problem (B.7) for the upper bound. The portfolio holds $v_1 = \frac{E_F(c(R))}{E_F(R)}$ dollars in the share and nothing in the bond. The portfolio has value C_n^u by construction, equivalent to the stated value in (28). To show that this portfolio satisfies the dual problem constraints, rewrite these inequalities in the manner above for the lower bound, using the inverse function J_n defined in (B.11) and the function H_n defined in (B.10). The revised constraints are

$$0 \geq H_n\left(J_n\left(\theta\right)\right) - v_1\theta - v_2, \theta \in \left(0, \frac{E_F\left(R\right)}{R_f}\right). \tag{B.24}$$

When evaluated using the candidate portfolio, this holds as an equality for extreme values of θ; using the limiting values in (B.13) and (B.12) we have

$$H_n\left(J_n\left(\theta\right)\right) - v_1\theta - v_2 \to 0 \text{ as } \theta \to 0 \text{ or } \frac{E_F\left(R\right)}{R_f}.$$

Because the compound function $H_n \circ J_n$ is convex for each $n \geq 2$, it follows that (B.24) holds.

Consider then the primal problem, and a series of functions y_i as candidates for y:

$$y_i(g) = \begin{cases} 1/R_f + a_i \text{ if } g < k_i \\ 1/R_f + b_i \text{ if } g \geq k_i \end{cases},$$

where the knots $k_i = K/i$, $i = 1, 2, ..$, are uniformly declining from the exercise price K, converging toward zero, and where the constants a_i, b_i are chosen to solve the constraints as equalities. Substituting y_i for y in (B.5) and (B.6) leads to

$$b_i = \frac{1 - E_F(R)/R_f}{E_F(R) - R_n(k_i)/I_n(k_i)} \underset{k_i \to 0}{\to} \frac{1}{E_F(R)} - \frac{1}{R_f}.$$

$$I_n(k_i)(b_i - a_i) = -b_i \underset{k_i \to 0}{\to} \frac{1}{R_f} - \frac{1}{E_F(R)}$$

Substituting y_i for y in (14) identifies the marginal utility associated with each y_i

$$m_n^i(r) = 1/R_f + b_i + (b_i - a_i) m_{n,k_i}(r) \underset{k_i \to 0}{\to} \frac{1}{E_F(R)}, \text{ for all } r \in (0, \infty).$$

As i increases, k_i declines to zero and $m_n^i(r)$ approaches the constant marginal utility $\frac{1}{E_F(R)}$ of a risk-neutral investor with linear utility.[24] Finally, substituting y_i for y in the primal objective (B.4) leads to

$$\begin{aligned} \overline{m} E_F(c(R)) + \int_{g=0}^{\infty} C_n(g)\, dy(g) &= (1/R_f + b_i) E_F(c(R)) + I_n(k_i)(b_i - a_i) \frac{C_n(k_i)}{I_n(k_i)} \\ &\underset{k_i \to 0}{\to} \frac{E_F(c(R))}{E_F(R)} \\ &= C^u \end{aligned}$$

Thus the primal objective is no less than C^u, where C^u is also the value of the objective of the dual identified above. Strong duality holds. QED

[24] We see $a_i, b_i < 0$ where $a_i = b_i(1 + 1/I_n(k_i)) \underset{k_i \to 0}{\to} -\infty$. However for each $r \in (0, \infty)$, $m_{n,k_i}(r) = 0$ for all $k_i \leq r$.

Appendix C Theorem 3

Theorem 3 is demonstrated in a roundabout fashion. To obtain the desired result we first show distribution F_{n+1} has greater risk than F_n, $n \geq 2$, in the sense of Rothschild and Stiglitz (RS, 1969). These authors demonstrate

Rothschild-Stiglitz - Greater Risk. For two distributions F_n and F_{n+1} with finite and equal means, $E_n(R) = E_{n+1}(R)$, the following statements are equivalent

$$\textit{(i)} \int_0^r (F_{n+1}(x) - F_n(x))\, dx \geq 0 \textit{ for all } r \in (0, \infty),$$

$$\textit{(ii)} \; E_{n+1}(f(R)) \geq E_n(f(R)) \textit{ for all convex functions } f : (0, \infty) \to \mathbb{R}.$$

Statement (i) says F_{n+1} puts more weight in the tails than F_n, while (ii) says the expectation of any convex function of R under F_{n+1} is greater than that under F_n. Each statement formally represents the idea that F_{n+1} has greater risk than F_n. We demonstrate that the risk-neutral distributions defined in (24) satisfy statement (i). Because call and put payoffs are convex in R, because statements (i) and (ii) are equivalent, and because a lower bound is the expected payoff under a distribution F_n, Theorem 3 holds. A lower bound is greater under F_{n+1} than F_n.

The demonstration of statement (i) is in turn simplified by an observation of Diamond and Stiglitz (DS, 1974): *If $E_n(R) = E_{n+1}(R)$, and if the distribution F_{n+1} crosses over F_n only once, then (i) holds.* Therefore our proof of Theorem 3 requires only a proof of

Proposition 3 - Single Crossing. For each $n \geq 2$, distribution F_{n+1} crosses over F_n once. This means a point $r^c \in (0, \infty)$ exists such that

$$\Delta_n(r) \stackrel{def}{=} F_{n+1}(r) - F_n(r) \begin{cases} > 0 & \text{if } 0 < r < r^c \\ = 0 & \text{if } r = r^c, \\ \leq 0 & \text{if } r^c < r < \infty. \end{cases} \tag{C.1}$$

Importantly, by the phrase F_{n+1} *crosses over* F_n we mean $\Delta_n(r) > 0$ (< 0) to the left (right) of r^c, as shown in (C.1), and not the reverse. Statement (i) of RS follows immediately from (C.1), implying risk-averse investors prefer distribution F_n over F_{n+1}.

Figures C.1(a) and C.1(b) demonstrate a single crossing, plotting the distributions F_3 and F_2 and their difference Δ_2, respectively. We see F_3 is above (below) F_2 for all $r < r_c$ ($> r_c$, respectively) where $r_c \simeq 1.045$. These distributions are constructed so that $E_3(R) = E_2(R) = R_f$, implying every risk averse investor $m \in \mathbf{M}_2$ prefers F_2 over F_3.

C.1 Difference in Distributions

To demonstrate (C.1), we analyse the difference $\Delta_n(r) = F_{n+1}(r) - F_n(r)$. The inequality $g_n < g_{n+1}$ (Lemma 3) together with the definition (24) imply

$$\Delta_n(r) < 0 \text{ for } r \in [g_n, g_{n+1}), \text{ and } \Delta_n(r) = 0 \text{ for } r = 0,\ r \in [g_{n+1}, \infty), \tag{C.2}$$

so we focus on the interval $(0, g_n)$. We show one and only one $r^c \in (0, g_n)$ satisfies (C.1).

The distributions F_n and F_{n+1} are continuous and strictly increasing on $(0, g_n)$, as is the physical distribution F. Thus, Δ_n is continuous. For $r \in (0, g_n)$

$$\begin{aligned} \Delta_n(r) &= \int_{x=0}^{r} \left(1 - \frac{dF_n(x)}{dF_{n+1}(x)}\right) dF_{n+1}(x) \\ &= \int_{x=0}^{r} \left(1 - B_n D_n(x)\right) dF_{n+1}(x), \end{aligned} \tag{C.3}$$

where if $n > 2$

$$B_n = \frac{I_{n+1}(g_{n+1})/g_{n+1}^{n-1}}{I_n(g_n)/g_n^{n-2}} = \frac{\int_{x=0}^{\infty}\left(1 - \frac{x}{g_{n+1}}\right)_+^{n-1} dF(x)}{\int_{x=0}^{\infty}\left(1 - \frac{x}{g_n}\right)_+^{n-2} dF(x)}, \text{ and } D_n(r) = \frac{\left(1 - \frac{r}{g_n}\right)_+^{n-2}}{\left(1 - \frac{r}{g_{n+1}}\right)_+^{n-1}}. \tag{C.4}$$

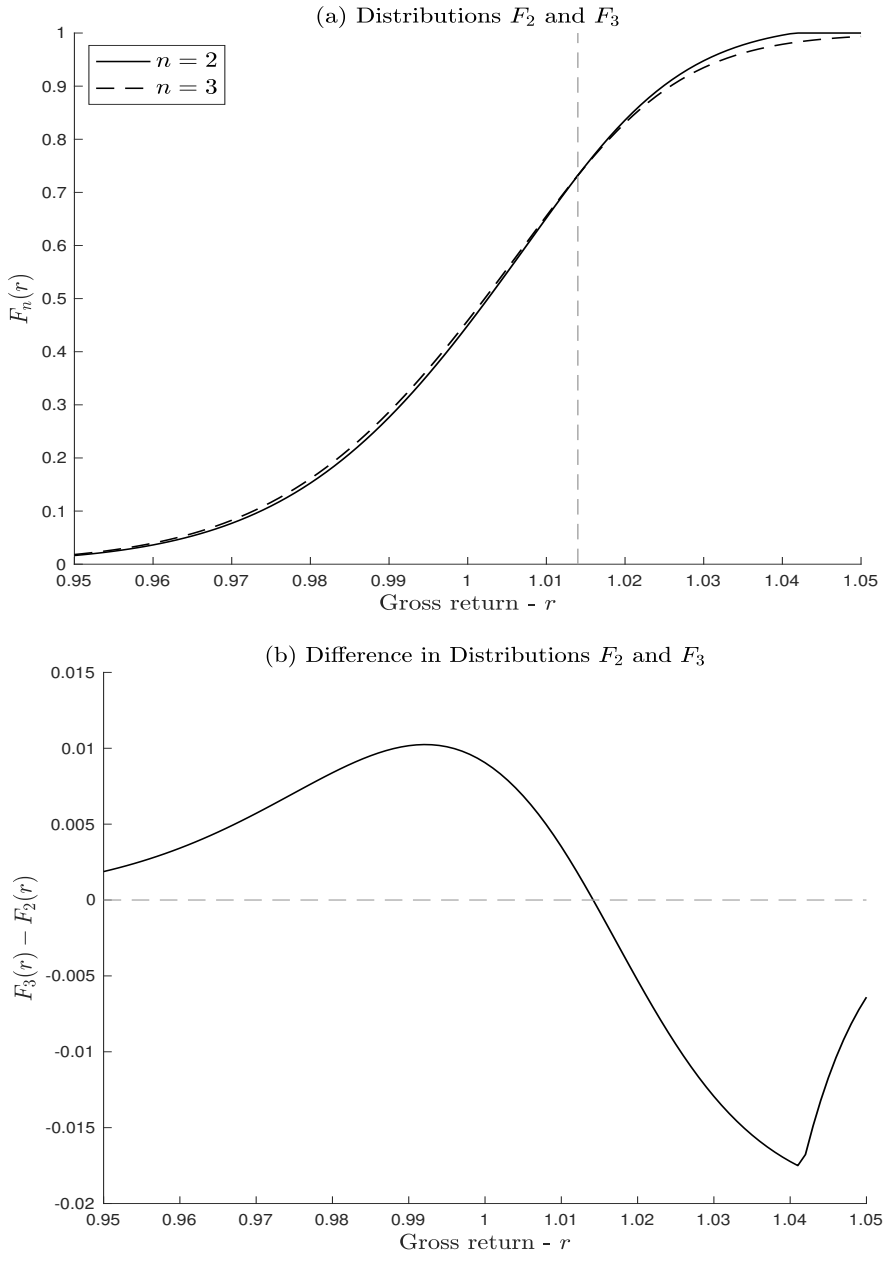
while if $n = 2$

$$B_2 = \frac{F(g_3) - \int_{x=0}^{g_3} \frac{x}{g_3} dF(x)}{F(g_2)} \text{ and } D_2(r) = \frac{g_3}{g_3 - r}. \tag{C.5}$$

Case $n = 2$ is treated separately because $D_2(r)$ is discontinuous at $r = g_2$; it is continuous and differentiable on the half-open interval $[0, g_n)$. For $n > 2$, D_n is continuous and differentiable on the closed interval $[0, g_n]$.

Figure C.1
Numerical Demonstration of Single Crossing

Notes: This figure illustrates the single crossing between the distributions F_2 and F_3. The distribution F is skewed t with moments given in the second column of Table 2. Figure (a) plots the distributions in levels, and a vertical line appears at the crossing point, $r = r^c$, where $\Delta_2(r) \stackrel{def}{=} F_3(r) - F_2(r) = 0$. To the left (right) of r^c, F_3 lies everywhere above (below) F_2. Figure C.1(b) plots the difference, $\Delta_2(r)$.



For all $n \geq 2$, the function D_n captures variation in increments $\frac{d\Delta_n(r)}{dF_{n+1}(r)}$ across $(0, g_n)$, where

$$D_n(0) = 1,\ D_n(g_n) = 0, \text{ and } D_n(r) > 0 \text{ for all } r \in (0, g_n),$$

while the constant $B_n > 0$ governs the sign of $\Delta_n(r)$ for r near zero. There exists $r_n^d \in (0, g_n)$ such that D_n is monotone increasing (decreasing) to the left (right, respectively) of r_n^d. To demonstrate this fact, consider the derivative of D_n on $(0, g_n)$,

$$D_n'(r) = \frac{d}{dr}\left(\left(\frac{1-\frac{r}{g_n}}{1-\frac{r}{g_{n+1}}}\right)^{n-2}\frac{1}{1-\frac{r}{g_{n+1}}}\right) = \begin{cases} \frac{g_3}{(g_3-r)^2} & \text{if } n=2 \\ \frac{\left(1-\frac{r}{g_n}\right)^{n-3}}{\left(1-\frac{r}{g_{n+1}}\right)^{n}}\frac{1}{g_{n+1}}\left(r_n^d - r\right) & \text{if } n>2, \end{cases}.$$

where

$$r_n^d = \begin{cases} g_n - (n-2)(g_{n+1}-g_n) < g_n & \text{if } n>2 \\ g_2 & \text{if } n=2. \end{cases} \tag{C.6}$$

For $n > 2$, r_n^d is the unique stationary point of maximum of D_n,

$$D_n'(r) \begin{cases} > 0, & r < r_n^d, \\ = 0, & r = r_n^d, \\ < 0, & r > r_n^d, \end{cases} \tag{C.7}$$

For $n = 2$, D_2 increases uniformly on $(0, g_2)$, $\lim_{r \uparrow g_2} D_2(r) = \frac{g_3}{(g_3-g_2)}$ is a supremum, but also D_2 is discontinuous at g_2 with $D_2(r) = 0$, $r \in [g_2, \infty)$. Thus $r_2^d = g_2$.

C.2 Single Crossing

Here we state and prove several lemmas, leading to Proposition 3. Lemma 4 shows $sign(\Delta_n)$ changes on the interval $(0, g_n)$, and there is at least one $r \in (0, g_n)$ at which the distributions cross with $\Delta_n(r) = 0$. Lemma 5 demonstrates that the signs of terms $1 - B_n$ and r_n^d jointly determine the sign of $\Delta_n(r)$ for r near zero, while Lemmas 6 and 7 together lead to the conclusion $\Delta_n(r) > 0$ for r near zero. In the proofs we rely on the inequalities of (C.7), and we rely on (C.3), which requires $sign\left(\frac{d\Delta_n(r)}{dF_{n+1}(r)}\right) = sign(1 - B_n D_n(r))$. The proof of Proposition 3 uses the lemmas to demonstrate (C.1).

Lemma 4. Neither distribution dominates the other. That is $\Delta_n(r) = 0$ *for some* $r \in (0, g_n)$, *and neither (4i)* $F_{n+1}(r) \geq F_n(r)$ *nor (4ii)* $F_{n+1}(r) \leq F_n(r)$, *holds for all* $r \in (0, g_n)$. *As a consequence* $1 - B_n D_n(r)$ *changes sign at least once on* $(0, g_n)$.

Proof: The inequalities (4i) contradict (C.2) so they cannot hold. Inequalities (4ii) and (C.2) together imply $E_{n+1}(R) > E_n(R)$, which contradicts the equality of means (26), so (4ii) cannot hold. Continuity leads us to conclude there exists $r \in (0, g_n)$ at which $\Delta_n(r) = 0$. If either $1 - B_n D_n(r) \geq 0$ or ≤ 0 for all $r \in (0, g_n)$ then one of the inequalities (4i) or (4ii) holds; in either case, we have again a contradiction. We conclude $1 - B_n D_n(r)$ changes sign on $(0, g_n)$. QED

Lemma 5. For $r \approx 0$, *sign* $(\Delta_n(r))$ *is determined by sign* $(1 - B_n)$ *and sign* $\left(r_n^d\right)$. *Specifically, for each* $n \geq 2$, *there exists* $\varepsilon_n > 0$, *such that for all* $r \in (0, \varepsilon_n)$,

$$\Delta_n(r) \begin{cases} > 0 & \text{if } 1 - B_n > 0 \text{ or } \left\{B_n = 1,\, r_n^d \leq 0\right\} \\ < 0 & \text{if } 1 - B_n < 0 \text{ or } \left\{B_n = 1,\, r_n^d > 0\right\}. \end{cases} \tag{C.8}$$

Proof: We demonstrate the result for $B_n = 1$ and $r_n^d \leq 0$. This case applies only if $n > 2$, and it allows $\varepsilon_n = g_n$. Other cases follow similarly. We have $B_n D_n(0) = 1$, and $B_n D_n$ is strictly decreasing on $(0, g_n)$ (per (C.7)). Hence for any $r \in (0, g_n)$

$$\begin{aligned} \Delta_n(r) &= \int_{x=0}^{r} (1 - B_n D_n(x))\, dF_{n+1}(x) \\ &> \int_{x=0}^{r} (1 - B_n D_n(0))\, dF_{n+1}(x) \\ &= 0. \end{aligned}$$

QED

Lemma 6. For each $n > 2$, $1 - B_n D_n(r)$ *and* $\frac{d\Delta_n(r)}{dF_{n+1}(r)}$ *change sign either only once or twice on the interval* $(0, g_n)$. *Furthermore if* $r_n^d \leq 0$, *they change sign only once.*

Proof. Lemma 4 requires $1 - B_n D_n(r)$ to change sign at least once on $(0, g_n)$. A monotonic function can cross zero only once. If $r_n^d > 0$, $1 - B_n D_n(r)$ is decreasing on $\left(0, r_n^d\right)$ and increasing on $\left(r_n^d, g_n\right)$ (see (C.7)). Therefore $1 - B_n D_n(r)$ may change sign twice, but no more. It may change

once on one or both of these intervals. If $r_n^d \leq 0$ then $1 - B_n D_n(r)$ is monotonically increasing on $(0, g_n)$, and to avoid dominance there must one (and only one) change of sign. QED

Lemma 7. $\Delta_n > 0$ *for* r *near zero. That is,* $\varepsilon_n > 0$ *exists such that* $\Delta_n(r) > 0$ *for all* $r \in (0, \varepsilon_n)$.

The proof of Lemma 7 shows $r_n^d > 0$ and $1 - B_n > 0$, and does so by ruling out all other possibilities. These inequalities together with Lemma 5 lead to the conclusion of Lemma 7.

Proof. Consider $sign\left(r_n^d\right)$. If $n = 2$ then $r_n^d = g_2 > 0$, so consider $n > 2$. Suppose $r_n^d \leq 0$. Lemma 4 says $1 - B_n D_n(r)$ changes sign once on $(0, g_n)$. Because $r_n^d \leq 0$ and $D_n'(r) \leq 0$ for all $r \geq r_n^d$ (see (C.7)), $1 - B_n D_n(r)$ is monotonically increasing on $(0, g_n)$. We consider now $sign(1 - B_n)$. *Case (7i).* If $r_n^d \leq 0$ and $1 - B_n \geq 0$ then $1 - B_n D_n(r) \geq 0$ uniformly on $(0, g_n)$. This contradicts Lemma 4. *Case (7ii).* If instead $r_n^d \leq 0$ and $1 - B_n < 0$ then Lemma 4 and monotonicity require a unique $r^z \in (0, g_n)$ such that

$$\frac{d\Delta_n(r)}{dF_{n+1}(r)} \begin{cases} < 0 & \text{if } 0 < r < r^z \\ = 0 & \text{if } r = r^z \\ > 0 & \text{if } r^z < r < g_n. \end{cases} \tag{C.9}$$

The first inequality implies $\Delta_n(r^z) < 0$. Lack of dominance (Lemma 4) requires a point r^c, $r^c > r^z$, at which $\Delta_n(r^c) = 0$. The final inequality of (C.9) says this point is unique, and implies $\Delta_n(g_n) > 0$. This contradicts (C.2).

The contradictions of cases (7i) and (7ii) lead us to conclude $r_n^d > 0$ for all $n \geq 2$. We use this fact in the following arguments.

Consider again $sign(1 - B_n)$, and suppose $1 - B_n \leq 0$. For all $n \geq 2$, (C.7) says $1 - B_n D_n(r) < 0$ for all $r \in \left(0, r_n^d\right)$, and this implies $\Delta_n\left(r_n^d\right) < 0$. We consider $n = 2$ and $n > 2$ separately. *Case (7iii).* If $n = 2$ then $r_n^d = g_n$ and $\Delta_n(g_n) < 0$ follows. This contradicts (C.2). *Case (7iv).* If instead $n > 2$ then $1 - B_n D_n(r)$ is increasing on $\left(r_n^d, g_n\right)$, which in turn implies (Lemma 6) that $r^z \in \left(r_n^d, g_n\right)$ exists such that (C.9) holds. To avoid dominance, there exists a point $r^c \in (r^z, g_n)$ such that (C.3) holds, implying $\Delta_n(g_n) = F_{n+1}(g_n) - F_n(g_n) \geq 0$. As this contradicts (C.2), we conclude again $1 - B_n > 0$.

In summary, we have shown by contradictions that $r_n^d > 0$ and $1 - B_n > 0$. It follows from Lemma 5 that $\varepsilon_n > 0$ exists such that for all $r \in (0, \varepsilon_n)$ QED

Finally we have

Proof of Proposition 3. Lemma 7 says $r_n^d > 0$ and $1 - B_n > 0$. Lemma 6 requires either one or two points on the interval $(0, g_n)$ at which $\frac{d\Delta_n(r)}{dF_{n+1}(r)}$ changes sign. Let one point be r^z, and assuming a second, let it be r^y, $r^z < r^y$. The monotonicity reported in (C.7) requires $r^z < r_n^d < r^y$, and

$$\Delta_n(r) \begin{cases} \text{increasing} & \text{if } 0 < r < r^z \\ \text{decreasing} & \text{if } r^z < r < r^y. \\ \text{increasing} & \text{if } r^y < r < g_n \end{cases} \tag{C.10}$$

where the final result holds assuming r^y exists. Lemma 4 requires a point $r^c \in (\, r^z, r^y)$ at which $\Delta_n(r) = 0$ and

$$\Delta_n(r) \begin{cases} > 0 & \text{if } 0 < r < r^c \\ < 0 & \text{if } r^c < r < r^y. \end{cases}$$

Point r^c must exist; otherwise F_{n+1} dominates F_n. Although $\Delta_n(r)$ is increasing to the right of r^y, it cannot cross zero twice; if it did, we would have $F_{n+1}(g_n) > F_n(g_n)$, which contradicts (C.2). Therefore, r^c is the unique point at which the distributions cross and (C.1) holds. QED

Appendix D Numerical Analysis

We assume log returns follow a skewed Student's t distribution (Hansen 1994), which is governed by parameters $\{\mu, \sigma, \lambda, \eta\}$, where the random gross return is

$$R = \exp(\mu + \sigma Z), \text{ with } \Pr(Z \leq z) = \int_{v=-\infty}^{z} f(v|\lambda, \eta),$$

with a density

$$f(z|\lambda,\eta) = \begin{cases} bc\left(1 + \frac{1}{\eta-2}\left(\frac{bz+a}{1-\lambda}\right)^2\right)^{-(\eta+1)/2} & \text{if } z < -a/b \\ bc\left(1 + \frac{1}{\eta-2}\left(\frac{bz+a}{1+\lambda}\right)^2\right)^{-(\eta+1)/2} & \text{if } z \geq -a/b \end{cases}$$

and subordinate parameters

$$a = 4\lambda c\left(\frac{\eta-2}{\eta-1}\right);\ b^2 = 1 + 3\lambda^2 - a^2;\ c = \Gamma\left(\frac{\eta+1}{2}\right)\Big/\left(\Gamma\left(\frac{\eta}{2}\right)\sqrt{\pi(\eta-2)}\right).$$

The mean and standard deviation of log returns are μ and σ, while $\lambda \in (-1, 1)$ and $\eta > 2$ jointly govern skewness and kurtosis.[25]

This distribution nests other familiar distributions. If $\lambda = 0$ the skewness of the log return is zero and follows a symmetric Student's t distribution with degrees of freedom η, and that distribution converges to the standard Gaussian as $\eta \to \infty$. Figure D.1 plots skewness abd kurtosis as functions of λ and η. We see the skewness of the distribution increases with λ, but at a rate that decreases with η. The kurtosis of the distribution increases with η, but at a rate that increases with λ. Skewness and kurtosis exist only when $\eta > 3$ and 4, respectively. There is a one-to-one relation betweeen pairs (λ, η) and {Skewness, Kurtosis}. This allows us to characterize the returns distribution in

[25] Jondeau and Rockinger (2003) demonstrate that the skewness $SK(R) = E_F\left(Z^3\right)$ and kurtosis $KT(R) = E_F\left(Z^4\right)$ of return are

$$SK(R) = \left(m_3 - 3am_2 + 2a^3\right)/b^3,$$

and

$$KT(R) = \left(m_4 - 4am_3 + 6a^2m_2 - 3a^4\right)/b^4,$$

where

$$m_2 = 1 + 3\lambda^2;$$
$$m_3 = 16c\lambda\left(1 + \lambda^2\right)\frac{(\eta-2)^2}{(\eta-1)(\eta-3)} \text{ if } \eta > 3;$$
$$m_4 = 3\left(1 + 10\lambda^2 + 5\lambda^4\right)\frac{(\eta-2)}{(\eta-4)} \text{ if } \eta > 4.$$

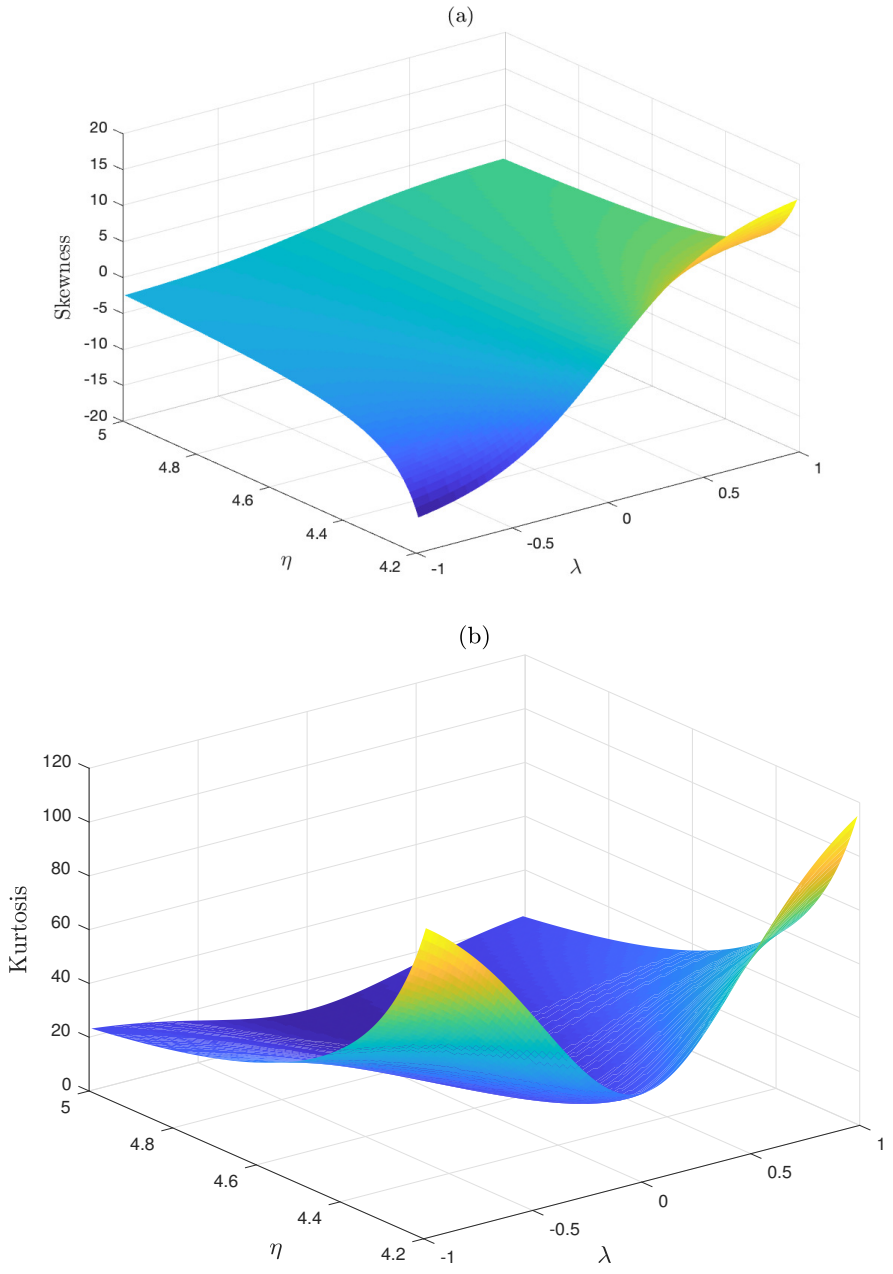
terms of these moments.

Figure D.1
Skewness and Kurtosis of skewed Student's t Distribution

Notes: This figure reports the skewness and kurtosis surfaces of the skewed Student's t distribution (Hansen 1994; Jondeau and Rockinger 2003):

$$SK(Z) = E_F\left(Z^3\right) = \left(m_3 - 3am_2 + 2a^3\right)/b^3$$
$$KT(Z) = E_F\left(Z^4\right) = \left(m_4 - 4am_3 + 6a^2m_2 - 3a^4\right)/b^4,$$

where $m_2 = 1 + 3\lambda^2$; $m_3 = 16c\lambda\left(1+\lambda^2\right)\frac{(\eta-2)^2}{(\eta-1)(\eta-3)}$ if $\eta > 3$; and $m_4 = 3\left(1 + 10\lambda^2 + 5\lambda^4\right)\frac{(\eta-2)}{(\eta-4)}$ if $\eta > 4$.



D.1 Data and Calibration

To establish baseline values of parameters of the skewed t distribution, we estimate the exponential GARCH (EGARCH) model of Nelson (1991) for weekly SPX price returns, Friday to Friday. Our data is from the Center for Research in Security Prices at the University of Chicago (CRSP). The sample period runs from January 1990 to December 2022. The start date mirrors the time SPX index options data became available, allowing comparison of our bounds to the existing literature.[26] We estimate an EGARCH(1,1) model:

$$\log(R_t) = a_0 + x_t,\ x_t = \sigma_t z_t,\ z_t \overset{i.i.d.}{\sim} f(z|\eta, \lambda) \tag{D.1}$$

$$\log(\sigma_{t+1}^2) = b_0 + b_1 z_t + b_2(|z_t| - E_F|z_t|) + b_3 \log(\sigma_t^2). \tag{D.2}$$

Parameter a_0 estimates a constant mean of log returns, while (b_1, b_2, b_3) govern the estimate of variance of weekly log returns σ_t^2.

Stochastic volatility loads differently on positive and negative lagged innovations in z_t, in addition to previous volatility realizations. We adopt a specification with single lags ($P = Q = 1$) for simplicity. The estimated parameters are baseline values used to calculate bounds on 1-week options.

We also perform a second estimation in which log returns are Gaussian ($\lambda = 0, \eta = \infty$). Table D.1 reports the EGARCH(1,1) estimates, while Table 2 reports the corresponding annualized conditional moments of the estimated distribution of log returns. The conditional mean of log returns, a_0, is between 12 and 13 basis points in each specification, which translates into a per annum expected return of approximately 6.5%. Consistent with the leverage effect documented by Nelson (1991) and others, b_1 is significantly negative in each estimation, as negative standardized return innovations z_t lead to higher future volatility in both the Gaussian and skewed t models. Estimates of λ and η imply that the weekly log returns distribution exhibits negative skewness (-0.507) and leptokurtosis (4.013).

The distribution's fit of the weekly returns data is statistically superior when it is permitted to deviate from the normal distribution. Several measures of fit are provided in Table D.1 and

[26] SPX options are: traded on the Chicago Board Option Exchange; European options (exercisable only at expiration); cash settled; and trade with times to expirations of one day to several years.

Table D.1
EGARCH(1,1) Parameter Estimates

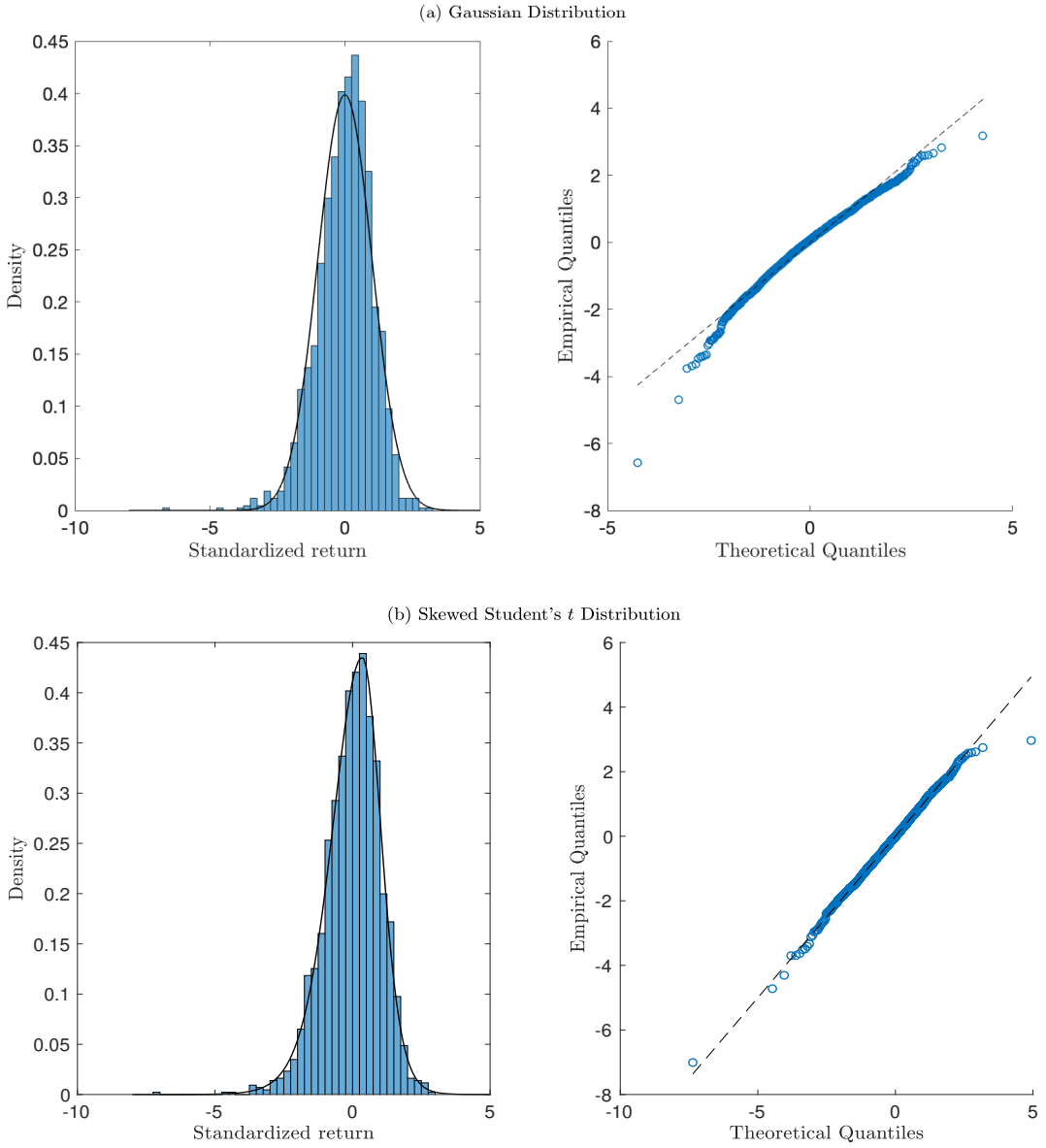
Notes: Parameter estimates from EGARCH(1,1) model using weekly log returns on the S&P 500 from January 1990–December 2022. Under the Gaussian, specification, log returns are assumed to follow the normal distribution, while under the skewed t distribution, they are assumed to follow a skewed Student's t distribution (Hansen 1994) with unconstrained (λ, η). Tests using the AIC and BIC indicate the skewed t distribution provides a significantly better fit of the data, while the smaller value of the Kolmogorov-Smirnov test statistic has a similar interpretation. Asymptotic standard errors are in parentheses. † indicates parameters are constrained, not estimated.

Parameter	Gaussian	Skewed t
a_0	0.00130 (0.000413)	0.00123 (0.000399)
b_0	-0.682 (0.103)	-0.565 (0.0992)
b_1	-0.193 (0.0223)	-0.199 (0.0237)
b_2	0.303 (0.0339)	0.245 (0.0340)
b_3	0.912 (0.0132)	0.928 (0.0127)
λ	$0.000^{\dagger}$	-0.232 (0.0347)
η	$\infty^{\dagger}$	11.776 (2.820)
Log-likelihood	4309.98	4354.00
AIC	-8610.00	-8694.00
BIC	-8582.70	-8655.80
Kolmogorov-Smirnov	0.0634***	0.0632***

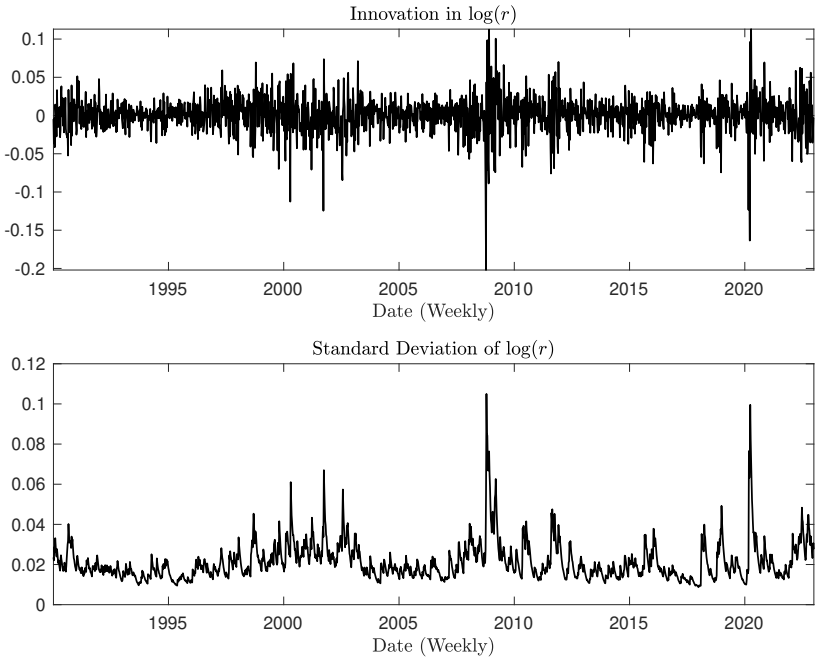
a visual representation is given in Figure D.2. Both the AIC and BIC demonstrate that the skewed t model performs better; the Kolmogorov-Smirnov test statistic is smaller in the skewed t model compared to the Gaussian model, although in each case the p-values lead to rejection of the null hypothesis that the underlying returns data come from the respective skewed Student's t distributions. Figure D.2 illustrates the fit by overlaying the estimated distributions on the weekly log returns data and the associated Q-Q plots. These figures confirm the Gaussian distribution is less likely to capture the extreme return realizations relative to the skewed t distribution. Time series of the innovation in and the stochastic volatility of log returns are portrayed in Figure D.2(c). As mentioned previously, the average conditional mean of weekly log returns, a_0, is 12 basis points, but there is significant variation over time generated by positive and negative innovations z_t. Likewise, the average conditional volatility of weekly log returns is 0.0212, with minimum and maximum values of 0.0087 and 0.105, respectively. Large spikes in volatility occur in 2008 and 2020, which coincide with large negative innovations in weekly log returns.

Figure D.2
EGARCH(1,1) Model Results

Notes: This figure reports the results from the EGARCH(1,1) model using weekly log returns on the S&P 500 from January 1990–December 2022. Panels (a) and (b) visualize the fit of the Gaussian and skewed t distributions to the underlying weekly log returns data, and panel (c) plots the time series of the innovations and volatility of log returns in the estimated skewed t model. Under the Gaussian specification, log returns are assumed to follow the normal distribution, while under the skewed t distribution, they are assumed to follow the skewed Student's t distribution (Hansen 1994) with unconstrained (λ, η).



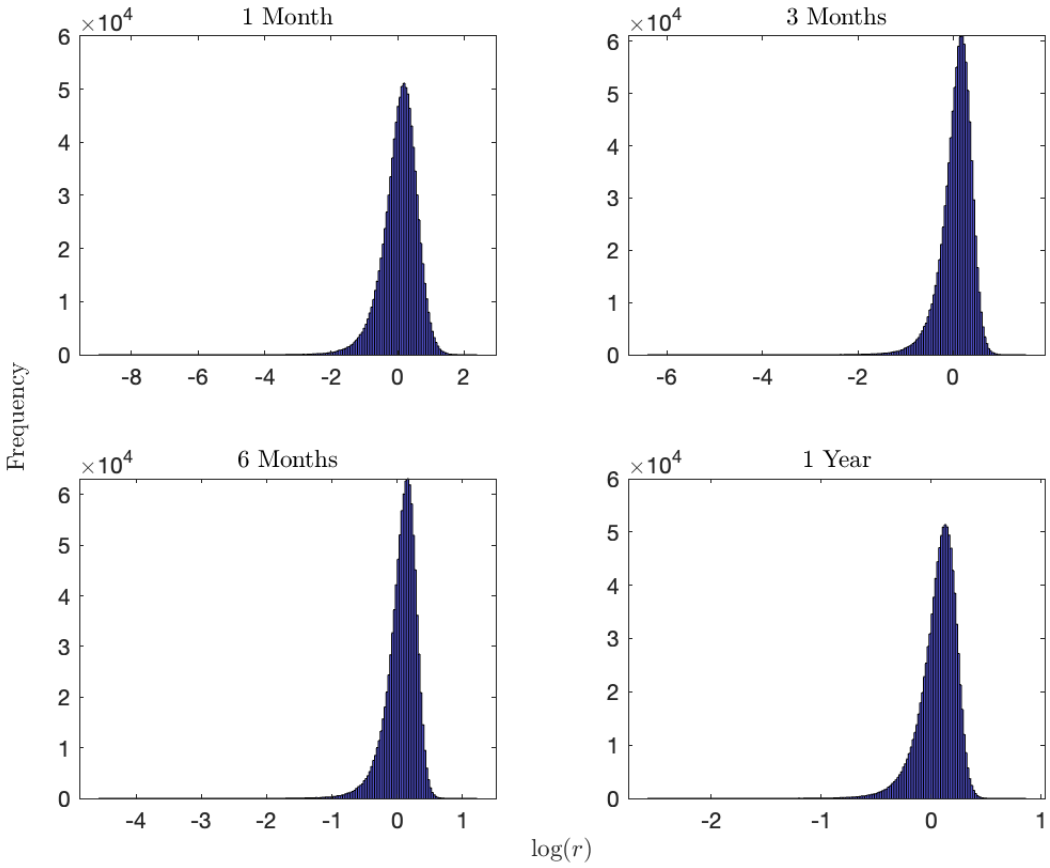
(c) Return Innovations and Stochastic Volatility



To calculate SD bounds for tenors longer than one week, we simulate weekly log returns using the estimated skewed t EGARCH(1,1) model discussed above. Specifically, we simulate one million sequences of 52 weekly log returns, $\left\{\{\log(R_t^s)\}_{t=1}^{52}\right\}_{s=1}^{10^6}$, where $\log(R_t^s)$ is a simulated weekly return given by the fitted equations (D.1) and (D.2), and then compound them to obtain (simulated) one-month, three-month, six-month, and one-year log returns. For a horizon T weeks, we compute $\log(R_{t,t+T}^s) = \sum_{t=1}^{T} \log(R_t^s)$. The histograms of the simulated returns are in Figure D.3, and their moments are in Table 2. As the return horizon T increases, the volatility of the distribution approaches its long-run mean, while the third and fourth moments are markedly more negatively skewed and leptokurtic due to the nature of the stochastic volatility process. Similarly to the weekly log returns, in our numerical analyses we assume these longer-horizon log returns follow a skewed Student's t distribution with the moments given in Table 2.

Figure D.3
Simulated Long-horizon Log Returns Distributions

Notes: This figure depicts histograms of the simulated returns data for one-month, three-month, six-month, and one-year log returns. Each distribution is the result of one-million simulated weekly skewed t log returns, appropriately compounded, where the simulated weekly returns use the parameter estimates from the EGARCH(1,1) model. The moments of the distributions are in Table 2.



D.2 Additional Numerical Results

In this section, we present several additional numerical results regarding the portfolios from the dual problem (9), and comparative statics of the stochastic dominance bounds with respect to the risk-free rate of interest.

D.2.1 Portfolios

The first-order conditions for the risky and risk-free assets in (4) and (5) are constraints in the primal problem (8). The Lagrange multipliers on these constraints, v_1 and v_2, in Theorem 2 appear in the dual problem (9) as portfolio positions in the risky and risk-free assets. The equalities (20) and (21) define these positions. Table D.2 reports the values of v_1 and v_2 for different degrees n and moneyness levels, K/S_0.

We highlight three patterns. First, for all n and moneyness levels K/S_0, the portfolios are highly levered, with $v_1 > 0$ and $v_2 < 0$. We define equity as $v_1 + v_2$, which is equal to C_n^l, and the margin level as $(v_1 + v_2)/v_1$. Overall, margin levels are much lower than the Reg T margin requirement of 50% in the United States. For every \$1 invested in the risky asset, only \$0.0009 to \$0.0363 is from equity, with the remaining \$0.9637 to \$0.9991 bought on margin.

Second, we find that for a given moneyness level K/S_0, equity and margin increase in the degree n, with larger differences between $n = 2$ and 3 than from $n = 3$ and 10. This result is economically reasonable. Finally, we find that for a given n, equity and margin are higher for the OTM calls and ITM puts than for the ITM calls and OTM puts. These changes are larger in magnitude than those induced by changes in n, and are due to the left-tail risk in the returns distribution, which pushes leverage and the risky share position down.

Table D.2
Call Option Dual Portfolios

Notes: Portfolio positions under the baseline calibration of the skewed t weekly returns distribution (column 2 of Table 2). The stock price S is normalized to 1. v_1 and v_2 are the dollar values in the risky share and risk-free asset. Equity $= v_1 + v_2$ and Margin $=$ Equity$/v_1$.

K/S_0	n	v_1^l	v_2^l	Equity^l	Margin^l	v_1^u	v_2^u	Equity^u	Margin^u
					$R_f = 0.025$				
0.97	2	0.976	-0.944	0.031	0.032	0.032	0	0.032	1
1.00	2	0.810	-0.802	0.008	0.010	0.009	0	0.009	1
1.03	2	0.276	-0.275	0.000	0.001	0.001	0	0.001	1
0.97	3	0.879	-0.847	0.032	0.036	0.032	0	0.032	1
1.00	3	0.472	-0.463	0.009	0.018	0.009	0	0.009	1
1.03	3	0.065	-0.064	0.001	0.009	0.001	0	0.001	1
0.97	10	0.869	-0.837	0.032	0.036	0.032	0	0.032	1
1.00	10	0.453	-0.445	0.009	0.019	0.009	0	0.009	1
1.03	10	0.059	-0.058	0.001	0.010	0.001	0	0.001	1
					$R_f = 0.0028$				
0.97	2	0.973	-0.942	0.031	0.032	0.032	0	0.032	1
1.00	2	0.791	-0.783	0.008	0.010	0.009	0	0.009	1
1.03	2	0.203	-0.203	0.000	0.001	0.001	0	0.001	1
0.97	3	0.879	-0.848	0.031	0.035	0.032	0	0.032	1
1.00	3	0.472	-0.463	0.008	0.018	0.009	0	0.009	1
1.03	3	0.065	-0.064	0.001	0.008	0.001	0	0.001	1
0.97	10	0.864	-0.833	0.031	0.036	0.032	0	0.032	1
1.00	10	0.446	-0.437	0.008	0.019	0.009	0	0.009	1
1.03	10	0.057	-0.056	0.001	0.010	0.001	0	0.001	1
					$R_f = 0.0528$				
0.97	2	0.980	-0.948	0.032	0.033	0.032	0	0.032	1
1.00	2	0.841	-0.832	0.009	0.010	0.009	0	0.009	1
1.03	2	0.393	-0.393	0.000	0.001	0.001	0	0.001	1
0.97	3	0.879	-0.847	0.032	0.036	0.032	0	0.032	1
1.00	3	0.472	-0.463	0.009	0.019	0.009	0	0.009	1
1.03	3	0.065	-0.064	0.001	0.009	0.001	0	0.001	1
0.97	10	0.874	-0.842	0.032	0.037	0.032	0	0.032	1
1.00	10	0.463	-0.454	0.009	0.019	0.009	0	0.009	1
1.03	10	0.062	-0.061	0.001	0.010	0.001	0	0.001	1

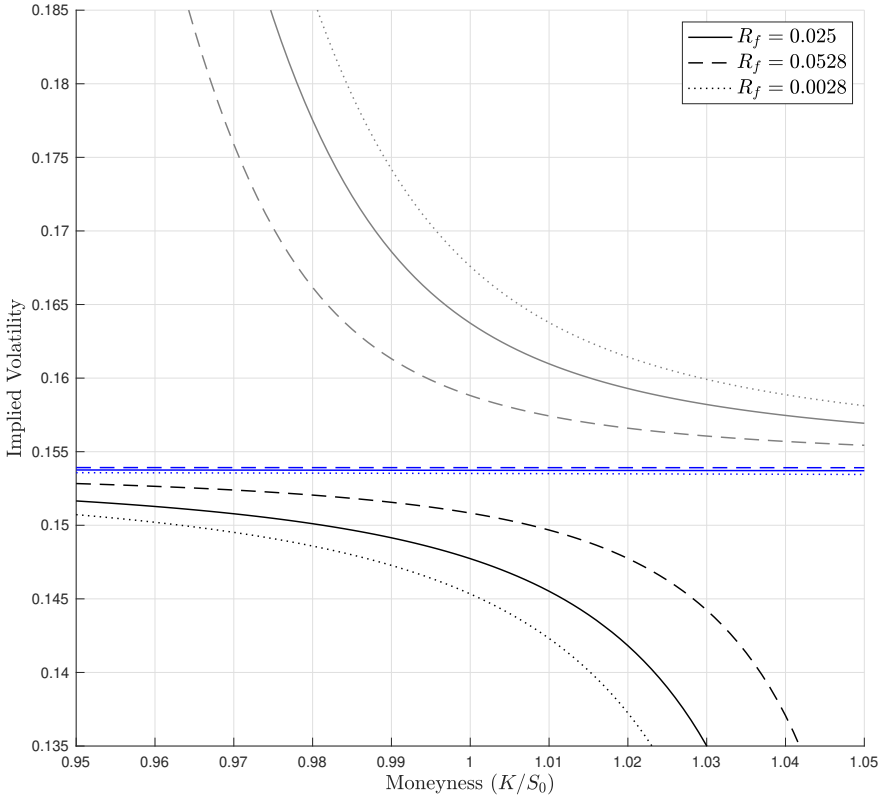
D.2.2 Risk-free rate

Figure D.4 plots the stochastic dominance bound implied volatilities on a weekly call option written on the SPX across different values of the risk-free rate, R_f. According to (28), and and consistent with Table D.2, the upper bound price, C^u, does not change with the risk-free rate. However, since the risk-free rate affects the present value of the strike price, the implied volatility associated with the price C^u is decreasing in R_f at a given moneyness level, K/S_0.

Although R_f decreases C_n^l directly in the denominator of (17), it also endogenously increases the equilibrium value g_n, which is the root of (18), leading to an increase in C_n^l. Altogether, an increase in R_f leads to a narrowing of the bounds on weekly call option IVs.

Figure D.4
Stochastic Dominance Bounds on Weekly SPX Call Option
Risk-free Rate

Notes: This figure reports comparative statics on the risk-free rate and the corresponding effects on stochastic dominance bounds on SPX call option prices. SPX log returns are assumed to follow a normal distribution. The conditional moments of this distribution are reported in the first column of Table 2. The black and blue lines are for the second and third-degree lower bounds, C_2^l and C_3^l, and the gray line is the upper bound, C^u. The lower and upper bounds are computed via (17) and (28). The baseline risk-free rate is set at 2.5% per annum.



Appendix E Comparison of SD and MDNA Bounds

We compare stochastic dominance bounds on option prices to the minimum-dispersion no-arbitrage bounds (MDNA) of Almeida and Freire (AF, 2022). Two primary differences between the bounds are discussed. One is the respective classes of investors. We search within a class $\mathbf{M}_n$ (defined in Section 2.2) to find SD bounds, while AF search within the class of HARA investors (their page 180). In each case, a bound is the value of an option using an investor's marginal utility as a discount factor. However neither a class $\mathbf{M}_n$ nor HARA is a strict subset of the other. For example, many HARA utility functions impose upper limits on wealth. In contrast, all investors in $\mathbf{M}_n$, $n \geq 2$, have utility functions defined on $(0, \infty)$. In addition, many of HARA investors are imprudent, preferring downside to upside risk, while all investors in $\mathbf{M}_n$, $n \geq 3$, are prudent.

The subclass of HARA investors that define MDNA upper bounds is a strict subset of $\mathbf{M}_n$, for all $n \geq 2$. As a consequence, an upper MDNA bound is never greater than the respective SD bound. In contrast, numerical analysis is required to determine which of the two lower bounds is tighter. Because the subclass of HARA investors that defines lower MDNA bounds includes imprudent investors, the theories do not order the respective lower bounds.

We also must consider different distributions of risky asset returns when calculating SD and MDNA bounds on option prices. AF calculate MDNA bounds assuming SPX returns follow the historical empirical distribution in their data.[27]. This choice of a discrete distribution is purposeful; it is necessary to bound wealth from above when calculating a MDNA lower bounds. Our theory assumes returns follow a continuously increasing distribution F on $(0, \infty)$; the estimation of F is described in Section 6 and Appendix D. We use distribution F for SD bounds and upper MDNA bounds, but to calculate MDNA lower bounds, we construct from F the continuous distribution

$$\overline{F}(r) = \frac{1}{F(\overline{r})} \int_{x=0}^{\overline{r}} dF(x),$$

where $\overline{r}$ is an upper limit such that $\overline{F}(r) = 1$. Using $\overline{F}$ allows us to consider imprudent HARA investors. We study values $\overline{r}$ in the right tail of F and satisfying $\overline{r} > R_f$, with the idea that $\overline{F}$ and F should be approximately the same. Numerical results show AF upper bounds vary only slightly across the values of $\overline{r}$ in the far right tail, but for $\overline{r}$ in the vicinity of the 99^{th} percentile of F, the

[27] They adjust for the level of recent realized variance of returns; see AF page 191.

MDNA lower bounds vary considerably. The free variable $\overline{r}$ must be chosen judiciously when a MDNA lower bound is calculated.

A SD bound on a call option with exercise price K is given by (27), and this is the solution to (B.4) subject to the first order conditions (B.5) and (B.6). A MDNA bound solves this problem, but with marginal utility chosen from the HARA class instead of $\mathbf{M}_n$. The first derivative of HARA utility at wealth w is

$$\frac{d}{dw}u^{\gamma}(w) = \begin{cases} a\gamma\left(b - a\gamma w\right)^{\frac{1}{\gamma}} & \text{if } \gamma \neq 0 \\ -\exp\left(-w\right) & \text{if } \gamma = 0 \end{cases}$$

where $\gamma \in (-\infty, \infty)$, $a > 0$ and $b - a\gamma w > 0$ are required. When $\gamma < 0$ or > 0, wealth must be bounded below or above, respectively,

$$\begin{array}{ll} w < \frac{b}{a\gamma} & \text{if } \gamma > 0 \\ w > \frac{b}{a\gamma} & \text{if } \gamma < 0 \end{array} \tag{E.1}$$

The Arrow-Pratt coefficient of risk aversion,

$$RA(w) = \frac{1}{b/a - \gamma w},$$

is increasing with γ, and is increasing or decreasing with wealth if $\gamma > 0$ or < 0, respectively. If $\gamma = 0$, wealth may be unlimited and utility is exponential with constant absolute risk aversion (CARA). The HARA investors with $\gamma \leq 1$ or > 1 are prudent or imprudent, respectively, and risk aversion declines to zero as $\gamma \to -\infty$ (See AF for further discussion.)

We calculate MDNA bounds within the setting of Section 2. A first-order condition identifies

α, the optimal investment in risky shares. If $\gamma < 0$, this is

$$\begin{aligned} 0 &= E_F\left(\frac{d}{d\alpha}u^{\gamma}(W)\right) \\ &= E_F\left(\left(b - a\gamma w_0\left(R_f + \alpha\left(R - R_f\right)\right)\right)^{\frac{1}{\gamma}} \times \left(R - R_f\right)\right) \\ &= \left(b - a\gamma w_0 R_f\right)^{\frac{1}{\gamma}} \times E_F\left(\left(1 - \frac{a\gamma w_0}{b - a\gamma w_0 R_f}\alpha\left(R - R_f\right)\right)^{\frac{1}{\gamma}} \times \left(R - R_f\right)\right) \\ &= E_F\left(\left(1 + x\left(R - R_f\right)\right)^{\frac{1}{\gamma}} \times \left(R - R_f\right)\right), \end{aligned} \tag{E.2}$$

where date T wealth is $W = w_0\left(R_f + \alpha\left(R - R_f\right)\right)$, and

$$x = -\frac{a\gamma w_0}{b - a\gamma w_0 R_f}\alpha. \tag{E.3}$$

If $\gamma = 0$ then CARA is used instead, and we solve

$$0 = E_F\left(\exp\left(1 + x\left(R - R_f\right)\right) \times \left(R - R_f\right)\right), \tag{E.4}$$

while if $\gamma > 0$, we solve (E.2) after substitution of distribution $\overline{F}$ or F. In each of these cases, a solution to the investor's problem is obtained by first finding x_γ to solve the *concentrated problem*, and then a solution to (E.3) is found for the optimal portfolio position α_γ.[28]

The logic of AF's Proposition 2 (in their online appendix) requires

$$\Pr\left(1 + x_\gamma\left(R - R_f\right) > 0\right) = 1$$

when $\gamma \neq 0$. This restriction imposes limits on x_γ, which in turn place bounds on γ, because x_γ is a continuous function of γ. In our setting under distribution F,

$$x_\gamma \in [0, 1/R_f] \tag{E.5}$$

is needed; because R is unlimited above, there is a positive likelihood $x_\gamma\left(R - R_f\right) < -1$ if either $x_\gamma < 0$ or $x_\gamma > 1/R_f$. Under the bounded distribution $\overline{F}$, the share return falls into the limited

[28] There is no need to report α_γ in our analysis. It is a function of the free parameters b, a and w_0, and is irrelevant to our conclusions.

range of outcomes $[0, \overline{r}]$, leading instead to the requirement

$$x_\gamma \in \left[-1/\left(\overline{r} - R_f\right), 1/R_f\right]. \tag{E.6}$$

AF demonstrate that the solution to equality (E.2) depends on $sign\left(\gamma\right)$: (i) if $\gamma < 0$ then $x_\gamma > 0$, while (ii) if $\gamma > 0$ then $x_\gamma < 0$. Furthermore, the magnitude $|x_\gamma|$ grows with $|\gamma|$, and as a consequence there is a feasible range $\left[\underline{\gamma}, \overline{\gamma}\right]$ outside of which (E.2) has no solution for γ. The endpoints $\underline{\gamma}$ and $\overline{\gamma}$ are *lower and upper MDNA bounds* for γ, respectively.

To find $\underline{\gamma}$, we solve (E.2) for γ having set $x = 1/R_f$, and using distribution F. We find $\overline{\gamma}$ similarly with $x = -1/\left(\overline{r} - R_f\right)$ and applying distribution $\overline{F}$. As the upper limit $\overline{r}$ in distribution $\overline{F}$ increases, the two intervals in (E.5) and (E.6) converge, and therefore the respective upper bounds $\overline{\gamma}$ converge. Alternatively as $\overline{r}$ declines, the difference $\overline{\gamma} - \underline{\gamma}$ grows, and our numerical analysis demonstrates this effect becomes demonstrably large as $\overline{r}$ approaches the 99^{th} percentile of distribution F.

There is tension in the choice of $\overline{r}$ in our numerical work, because the marginal value of an option to a HARA investor declines with γ. As a consequence, the lower MDNA bound on an option price is defined by the investor with $\gamma = \overline{\gamma}$, and this investor's evaluation depends on the distribution $\overline{F}$ and the upper limit $\overline{r}$. On the one hand, $\overline{r}$ should be large so the distributions $\overline{F}$ and F differ only a bit, but in this case the range between the upper and lower MDNA bounds on option prices on is small. On the other hand, if the bound $\overline{r}$ is modest, say near the 99^{th} percentile, then the range of option prices is larger. Again, $\overline{r}$ must be chosen judiciously as it governs the range between lower and upper MDNA bounds

E.1 Option Bounds

We follow AF's steps to establish MDNA bounds on option prices. For each exercise price K on a grid surrounding $K/S_0 = 1$, the value of the option, say, C_γ is found using the risk neutral distribution. For $\gamma < 0$ this value is

$$C_\gamma = \frac{1}{R_f} \frac{E_F\left(\left(1 - x_\gamma \frac{1}{R_f}\left(R - R_f\right)\right)^{\frac{1}{\gamma}} \times \left(R - K\right)_+\right)}{E_F\left(\left(1 - x_\gamma \frac{1}{R_f}\left(R - R_f\right)\right)^{\frac{1}{\gamma}}\right)}. \tag{E.7}$$

where x_γ is the solution to the concentrated problem. In the case $\gamma = 0$ CARA marginal utility is used in (E.7), and if $\gamma > 0$ the bounded distribution $\overline{F}$ is used. Finally, for each K we search across the grid of C_γ, and the largest and smallest values are chosen as the upper and lower MDNA bounds, $C_{\underline{\gamma}}$ and $C_{\overline{\gamma}}$, respectively, on the option price. We find the upper and lower bounds on option prices are associated with the *lower and upper* bounds of γ, respectively. Higher risk aversion leads to a lower option value.

E.2 Numerical Comparison of SD and MDNA Bounds

Upper and lower MDNA bounds on prices are very tight for the weekly options; they are nearly indistinguishable using the baseline parameters of our numerical analysis. Furthermore, they are nearly equal to the lower SD bounds for degrees $n \geq 3$.

Figure E.1 demonstrates these facts. In Figure E.1(a) are the upper and lower MDNA bounds together with the upper SD bound and the lower 3^{rd}-degree bounds. This figure can be compared to Figure 1(b), except that the lower 2^{nd} and 10^{th}-degree SD bounds are not shown here, while MDNA bounds are shown. The upper SD bound is easily seen; it is clearly above the others. The other three bounds appear to lie on top of each other. Thus there is little difference between the two MDNA bounds, and the 3^{rd}-degree bound appears equivalent to each of them.

Figure E.1(b) provides additional clarity. It represents the same data, but over a much smaller range of near the money options, $K/S_0 \in [0.9995, 1.00005]$, and a smaller range of implied volatility. The upper SD bound is excluded from this figure, and only the two MDNA and the lower 3^{rd}-degree bounds are shown. Now the upper MDNA bound is clearly above and separated from the two lower bounds, while the two lower bounds again overlay each other. However, upper bound differs from the other two only in the fourth decimal point of implied volatilities, while the SD and MDNA lower bounds appear to be identical.

A numerical example is in Table E.1. We see four values of the upper limit on returns $\overline{r}$ in distribution $\overline{F}$, together with respective probabilities in the upper tail, $\Pr_F(R \geq \overline{r})$ under distribution F, and lower MDNA bounds. Again, baseline parameter values and weekly options are used in these calculations, and bounds are shown as Black-Scholes IVs. The bounds in the table are for the at-the-money option, and they may be compared to the lower SD bound, which is 0.1518.

Figure E.1
Comparison of SD and MDNA Bounds

Notes: This figure plots the implied volatilities associated with the minimum dispersion no arbitrage (MDNA) bounds (Almeida and Freire 2022) on a weekly SPX call option. The SD bounds are also plotted for reference. SPX log returns are assumed to follow a skewed t distribution. The conditional moments of this distribution are in the second column of Table 2.

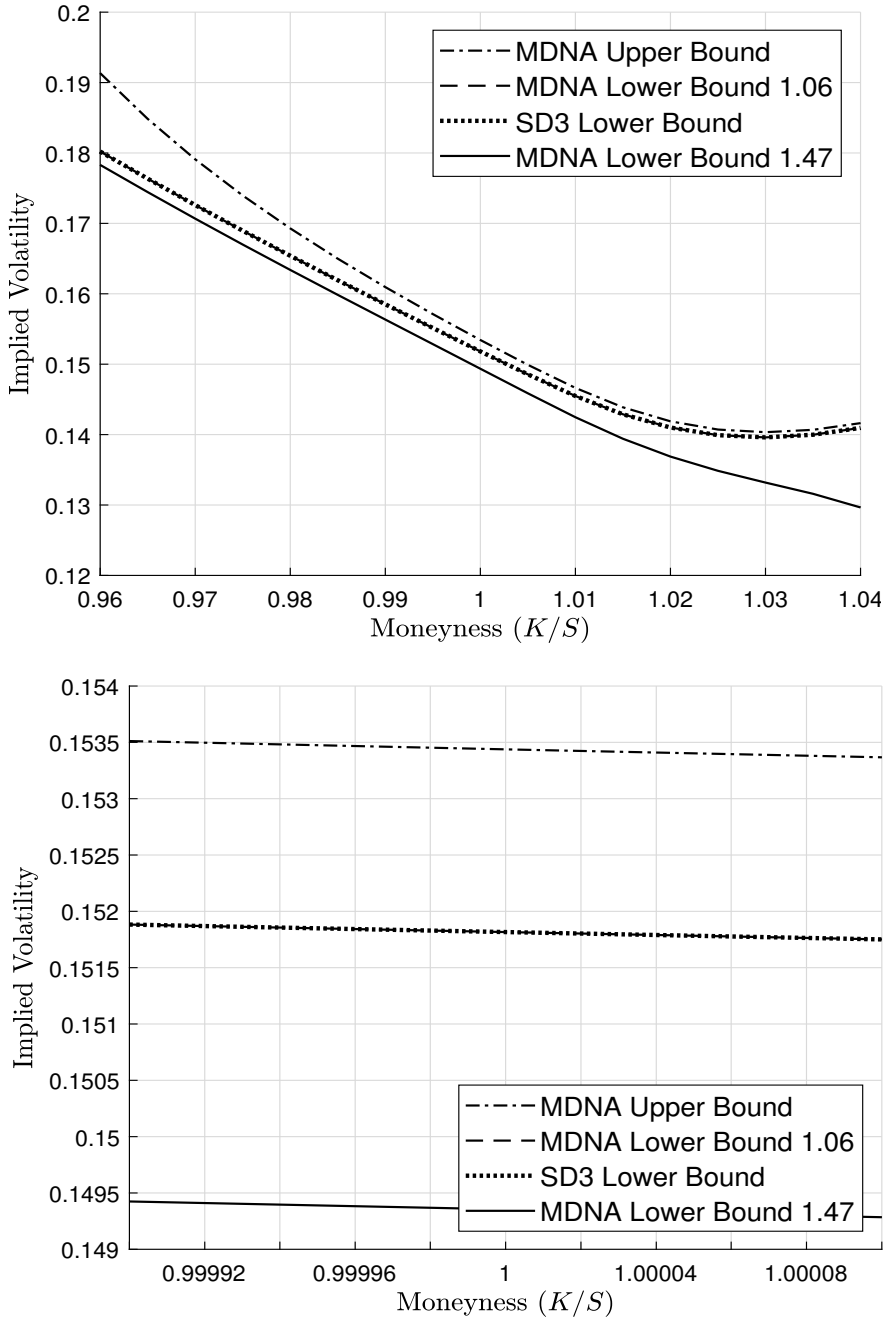


Table E.1
Tail Probabilities and Lower MDNA Bounds on Call Option Prices

$\overline{r}$	$\Pr_F(R \geq \overline{r})$	*Lower MDNA Bound* $(K/S_0 = 1)$
1.0575	30 *b.p.*	0.1494
1.0669	10	0.1502
1.0881	1	0.1509
1.4642	4.77×10^{-8}	0.1518

The tail probabilities are shown in basis points and are small, with the largest value of 30 b.p. corresponding to a weekly return on the SPX of 5.75%, which is 2.44 standard deviations above the mean of weekly log returns. The smallest value at the bottom of second column represents the probability in the tail of the distribution above $g_3 = 1.4642$; this value defines the investor who represents the third-degree lower bound (equation (18)). The difference between the distributions F and $\overline{F}$ declines as $\overline{r}$ increases, but at the same time, the MDNA lower bound in the third column rises, at first sharply and then mildly, with more than half of the difference between 0.1494 and 0.1518 accounted for by a rise in $\overline{r}$ from 1.0575 to 1.0881. In the extreme case for very large $\overline{r}$, the lower MDNA and SD appear to be identical.

These results in our baseline case for very short-tenor SPX options suggest that lower n^{th}-degree SD bounds for $n \geq 2$ are a good substitute for lower MDNA bounds, and vice versa. These alternatives are difficult to distiguished from one another. Furthermore if the distributions F and $\overline{F}$ are nearly the same, the MDNA bounds establish a narrow range between upper and lower bounds. Future analysis will study alternative distributions for the risky return and alternative tenors of options.

References

[1] Almeida, Caio and Gustavo Freire, 2022, Pricing of Index Options in Incomplete Markets, *Journal of Financial Economics* 144, 174-205

[2] Almeida, Caio and Gustavo Freire, 2023, Demand in the Option Market and the Pricing Kernel, Working Paper.

[3] Arrow, Kenneth, 1965, *Aspects of the Theory of Risk Bearing*, Helsinki: Yrjö Jansonin Säätiö.

[4] Arrow, Kenneth, 1970, Essays in the Theory of Risk-Bearing, Amsterdam: North-Holland.

[5] Bakshi, Gurdip, Nikunj Kapadia, and Dilip Madan, 2003, Stock Return Characteristics, Skew Laws, and the Differential Pricing of Individual Equity Options, *Review of Financial Studies* 16, 101–143.

[6] Bawa, Vijay, 1975, Optimal Rules for Ordering Uncertain Prospects, *Journal of Financial Economics* 2, 95 - 121.

[7] Bernardo, A. and O. Ledoit, 2000, Gain, Loss, and Asset Pricing, *Journal of Political Economy* 108, 144-172.

[8] Bollen, N. P. B. and R. E. Whaley, 2004, Does Net Buying Pressure Affect the Shape of Implied Volatility Functions?, *Journal of Finance* LIX, 711-753..

[9] Carr, Peter and Dilip Madan, 1998, Towards a Theory of Volatility Trading, In: *Volatility: New Estimation Techniques for Pricing Derivatives*, Jarrow (ed.), Vol. 29. Risk Books, pp. 417-427.

[10] Cochrane, J. H. and Jesús Saá-Requejo, 2000, *Journal of Political Economy* 108, 79-119.

[11] Constantinedes, George M. and Stylianos Perrakis, 2002, Stochastic Dominance bounds on Derivatives Prices in a Multiperiod Economy with Proportional Transaction Costs, *Journal of Economic Dynamics & Control* 26, 1323-1352.

[12] Constantinedes, George M., and Stylianos Perrakis, 2006, Stochastic Dominance Bounds on American Option Prices in Markets with Frictions, Review of Finance 10, 1-43.

[13] Constantinedes, George M., Jens Carsten Jackwerth, and Stylianos Perrakis, 2008, Mispricing of S&P 500 Index Options, Review of Financial Studies, 1248-1277.

[14] Denuit, Michel M. and Louis Eeckhoudt, 2010, Stronger Measures of Higher-Order Risk Attitudes, *Journal of Economic Theory* 145, 2027-2036.

[15] Derman, Emanuel and Michael B. Miller, 2016, *The Volatility Smile*, John Wiley & Sons, Inc., Hoboken, New Jersey.

[16] Diamond, Peter A. and Joseph E Stiglitz, 1974, Increases in Risk and it Risk Aversion, *Journal of Economic Theory* 8, 337-360.

[17] Eeckhoudt, Louis and Harris Schlesinger, 2006, Putting Risk in Its Proper Place, *American Economic Review* 96, 280-289.

[18] Ekern, Steinar, 1980, Increasing Nth Degree Risk, *Economic Letters* 6, 329-333.

[19] Garleanu, Nicolae, Lasse Heje Pedersen and Allen M. Poteshman, 2011, Demand-Based Option Pricing, Review of Financial Studies 22, 4259-4299.

[20] Hadar, J. and W. Russell, Rules for ordering uncertain prospects, American Economic Review 59, 25-34.

[21] Hansen, Bruce E., 1994, Autoregressive Conditional Desnsity Estimation, International Economic Review 35, 705-730.

[22] Jondeau, Eric and Michael Rockinger, 2003, Conditional volatility, skewness and kurosis: existence, persistence, and comovements, *Journal of Economic Dynamics and Control* 27, 1699-1737.

[23] Levy, Haim, 1985, Upper and Lower Bounds of Put and Call Option Value: Stochastic Dominance Approach, *Journal of Finance* XI, 1197-1217.

[24] Levy, Haim, 2016, *Stochastic Dominance: Investment Decision Making Under Uncertainty*, Springer.

[25] Mathur, K., and P. Ritchken, 1999, Minimum Option Prices Under Decreasing Absolute Risk Aversion, *Review of Derivatives Research* 3, 135-156.

[26] Menezes, C., C. Geiss, and J. Tressler, 1980, Increasing Downside Risk, *The American Economic Review* 70, 921-932.

[27] Nelson, Daniel B., 1991, Conditional Heteroskedasticity in Asset Returns: A New Approach, *Econometrica* 59, 347-370.

[28] Neuberger, Anthony and Richard Payne, 2021, The Skewness of the Stock Market over Long Horizons, *Review of Financial Studies* 34, 1572-1616.

[29] Perrakis, Stylianos and Peter J. Ryan, 1984, Option Pricing Bounds in Discrete Time, *Journal of Finance* XXXIX, 519-525.

[30] Perrakis, Stylianos, 2019, *Stochastic Dominance Option Pricing*, Palgrave Macmillan.

[31] Post, Thierry, 2003, Empirical Test for Stochastic Dominance Efficiency, *Journal of Finance* 58, 1905-1931.

[32] Pratt, John, 1964, Risk Aversion in the Small and the Large, *Econometrica* 32, 122-136.

[33] Quirk, J. P. and R. Saposnik, 1962, Admissibility and Measurable Utility Functions, *Review of Economic Studies* 29, 140-46.

[34] Ritchken, Peter H., 1985, On Option Pricing Bounds, *Journal of Finance* XL, 1219-1233.

[35] Ritchken, P. and S. Kuo, 1989, On Stocastic Dominance and Decreasing Absolute Risk Averse Option Pricing Bounds, *Management Science* 35, 51-59.

[36] Ross, S., 1978, A Simple Approach to the Valuation of Risky Streams, *Journal of Business* 51, 453-475.

[37] Rothschild, M. and J.E. Stiglitz, 1970, Increasing Risk, *Journal of Economic Theory* 2, 225-243.

[38] Rubinstein, M., 1976, The Valuation of Uncertain Income Streams and the Pricing of Options, *The Bell Journal of Economics* 7, 407-425.

[39] Williamson, R. E., 1956, Multiply Monotone Functions and Their Laplace Transforms, *Duke Mathematics Journal* 23, 189–207.